9226 *Biochemistry* **2010,** *49,* 9226–9240
DOI: 10.1021/bi101134h

BIOCHEMISTRY
including biophysical chemistry & molecular biology
Article

Distance Measurements within a Concatamer of the Plasma Membrane Cl^-/HCO_3^- Exchanger, AE1[†]

Arghya Basu,[‡] Shirley Mazor,[‡] and Joseph R. Casey*

Membrane Protein Research Group, Department of Physiology and Department of Biochemistry, School of Molecular and Systems Medicine, 721 Medical Sciences Building, University of Alberta, Edmonton, Alberta, Canada T6G 2H7.
[‡]*These authors contributed equally to this work.*

Received July 16, 2010; Revised Manuscript Received September 8, 2010

ABSTRACT: AE1, which exists in the erythrocyte plasma membrane as a noncovalent dimer, facilitates transmembrane Cl^-/HCO_3^- exchange. Here a concatamer of AE1 (two AE1 monomers fused via a two-residue linker to form an intramolecular dimer) was designed to facilitate fluorescence resonance energy transfer (FRET) studies. The concatameric protein (AE1·AE1) was expressed at the plasma membrane at levels similar to that of wild-type AE1 and had Cl^-/HCO_3^- exchange activity indistinguishable from that of wild-type AE1. Nondenaturing gel electrophoresis revealed that AE1·AE1 does not associate into higher-order oligomers when expressed in HEK293 cells and *Xenopus laevis* oocytes. The cysteine-less concatamer (AE1·AE1-C$^-$) enabled introduction of unique cysteine residues into the whole intramolecular dimer. AE1(Q434C)·AE1(Q434C)-C$^-$, with a single cysteine residue in each AE1 subunit, was labeled with the donor Alexa Fluor 488 C_5-maleimide (AF) and the acceptor tetramethylrhodamine methanethiosulfonate (TMR-MTS). Energy transfer efficiency revealed that the distance between these residues in the AE1 dimer is 49 ± 5 Å. The 72% FRET efficiency observed between AE1(Q434C)·AE1-C$^-$ labeled with AF and the lipid bilayer labeled with 1,1′-didodecyl-3,3,3′,3′-tetramethylindocarbocyanine perchlorate indicates that Q434 is less than 33 Å from the lipid bilayer. We thus provide two distance constraints for the position of Q434, which is located in extracellular loop 1, connecting the first two transmembrane segments of AE1.

The most abundant integral membrane protein in the human erythrocyte is anion exchanger 1 (AE1),[1] also called Band 3 or SLC4A1 (*1*), which facilitates exchange of chloride for bicarbonate ions across the plasma membrane. This electroneutral process increases the carbon dioxide carrying capacity of blood (*2*). The second function of AE1 in the erythrocyte is to provide the mechanical linkage between the membrane and the cytoskeleton to maintain the proper shape and flexibility of the erythrocyte (*3*−*5*). An alternate transcript of AE1, kAE1, is expressed only in the basolateral membrane of α-intercalated cells of the renal collecting duct, where it facilitates reabsorption of HCO_3^- (*2*).

AE1 forms dimers (*6*); however, previous studies demonstrated that each AE1 monomer unit exhibits independent exchange activity (*7*). Full-length AE1 protein consists of 911 amino acids, forming two major domains: a 43 kDa N-terminal cytoplasmic domain and a 55 kDa C-terminal membrane domain. Although a high-resolution crystal structure has been reported for the cytoskeletal interacting N-terminal domain (*8*), no high-resolution structure of the C-terminal membrane domain is available, which alone is able to facilitate ion exchange (*2*). Studies of AE1 topology (*9*−*14*) provided information about the transmembrane segments, the extracellular and intracellular regions of the exchanger. This led to the understanding that the membrane domain has 12−14 transmembrane segments (*15*), which are important for anion exchange. The membrane domain, with dimensions of 60 Å × 110 Å, has a central depression that has been visualized by an electron micrograph of negatively stained two-dimensional crystals (*16*). Recent electron microscopy (EM) studies have provided a projection map of the membrane domain at 7.5−16 Å resolution (*17*), but all the transmembrane segments could not be visualized in the projection map.

Conformational rearrangements are a feature of membrane transport protein mechanisms (*18*−*24*). AE1 transports up to 10^5 anions per second (*25*), a rate 100−1000-fold higher than the rates of other membrane transport proteins. Unique conformational rearrangements may be part of the AE1 anion transport mechanism, explaining the high turnover rate. The large volume of activation found for AE1 (*26*) and chemical labeling experiments (*27*) are suggestive of widespread conformational changes in the protein. EM structural data from two-dimensional crystals (*16*) and alternate accessibility of the K743 residue (*14*, *28*) also suggest that AE1 may experience significant conformational

[†]This work was supported by an operating grant from the Canadian Institutes of Health Research. J.R.C. is a scientist of the Alberta Heritage Foundation for Medical Research (AHFMR), and A.B. is a postdoctoral fellow of AHFMR.

*To whom correspondence should be addressed: Membrane Protein Research Group, Department of Physiology and Department of Biochemistry, School of Molecular and Systems Medicine, 721 Medical Sciences Building, University of Alberta, Edmonton, Alberta, Canada T6G 2H7. Phone: (780) 492-7203. Fax: (780) 492-8915. E-mail: joe.casey@ualberta.ca.

[1]Abbreviations: AE1, anion exchanger 1; AF, Alexa Fluor 488 C_5-maleimide; BCECF, 3′,6′-bis(acetyloxy)-5(or 6)-{[(acetyloxy)methoxy]-carbonyl}-3-oxospiro[isobenzofuran-1(3*H*),9′-[9H]xanthene]-2′,7′-dipropanoic acid 2′,7′-bis[(acetyloxy)methyl] ester; $DiIC_{12}$(3), 1,1′-didodecyl-3,3,3′,3′-tetramethylindocarbocyanine perchlorate; EC, extracellular loop; FRET, fluorescence resonance energy transfer; MBM, modified Barth's medium; PVDF, polyvinylidene fluoride; TM, transmembrane segment; TMR-MTS, 2-{[5(6)-tetramethylrhodamine]carboxylamino} ethyl methanethiosulfonate.

 Published on Web 09/09/2010

changes during ion transport. To date, little is understood regarding the nature of these conformational changes. A model for the monovalent anion exchange of AE1 proposes that the protein follows "ping-pong" kinetics, in which substrate anions cross the membrane one at a time and distinct inward or outward conformations are formed (*29*).

We have developed a system for revealing distances between transmembrane segments of human AE1 and for examining conformational changes associated with transport activity, using fluorescence resonance energy transfer (FRET). During FRET, fluorescence energy is transferred from a donor to an acceptor fluorophore. When a donor fluorescence probe is excited, its energy can be absorbed by an acceptor probe if it is in the proximity of the donor (typically 10−100 Å). The donor−acceptor energy transfer leads to a decrease in donor fluorescence intensity, a decrease in the donor excited state lifetime, and an increase in the acceptor's emitted fluorescence. The efficiency of energy transfer is inversely dependent upon the sixth power of the distance between the donor and acceptor as shown by Förster (Förster distance) (*30*). This property can be exploited to report on distances within the scale of biological macromolecules (*31*).

The main challenge in using FRET is the dimeric nature of AE1. The minimal oligomeric state of AE1 is dimeric (*6*); AE1 monomers are strongly associated within the dimeric unit, such that denaturation is required to dissociate them (*32*). If a fluorescent FRET probe is introduced into AE1, there will be a second probe within 110 Å [the length of an AE1 dimer (*16*)] on the second subunit of the dimeric unit. To overcome this problem, we designed a concatameric version of AE1 with two AE1 monomers fused into an intramolecular dimer. This enables the control of positions of any desired site-directed mutations in the dimeric form. In these studies, a cysteine-less version of AE1, called AE1-C$^-$ (*33*), was used. AE1-C$^-$ has been characterized as being functionally active (*33*) and has been used for protein chemical studies (*34*). Use of AE1-C$^-$ enables insertion of new cysteine mutations into a background that otherwise lacks cysteine. Using specific cysteine-directed protein chemistry allows fluorescent probes to be directed to unique cysteine sites.

In this study, an AE1 concatamer (AE1·AE1) was constructed and expressed in human embryonic kidney (HEK293) cells and *Xenopus laevis* oocytes. We demonstrate that the concatameric protein is processed to the plasma membrane and is as functional as the wild-type monomeric AE1. Site-directed labeling of two mutated Q434C residues in each monomeric unit of the cysteine-less AE1 concatamer was exploited to measure the distance between two transmembrane segments across the dimeric interface. A single Q434C mutation in AE1·AE1-C$^-$ was used to investigate the proximity of this residue to the lipid bilayer.

MATERIALS AND METHODS

Materials. 1,1′-Didodecyl-3,3,3′,3′-tetramethylindocarbocyanine perchlorate [DiIC$_{12}$(3)] and Alexa Fluor 488 C$_5$-maleimide (AF) were purchased from Molecular Probes (Carlsbad, CA). 2-{[5(6)-Tetramethylrhodamine]carboxylamino} ethyl methanethiosulfonate (TMR-MTS) was purchased from Toronto Research Chemicals (North York, ON). Pfx DNA polymerase, Dulbecco's modified Eagle's medium (DMEM), fetal bovine serum, calf serum, penicillin-streptomycin-glutamine, Alexa Fluor 488 chicken anti-mouse IgG, and 3′,6′-bis(acetyloxy)-5(or 6)-{[(acetyloxy)methoxy]-carbonyl}-3-oxospiro[isobenzofuran-1(3*H*),9′-[9H]xanthene]-2′,7′-dipropanoic acid 2′,7′-bis[(acetyloxy)methyl] ester (BCECF-AM) were obtained from Invitrogen (Carlsbad, CA). Poly-L-lysine, Igepal CA-630, and nigericin were from Sigma-Aldrich (Oakville, ON). Restriction enzymes were from New England Biolabs (Ipswich, MA). Oligonucleotides were from Integrated DNA Technologies (Coralville, IA). ECL enhanced chemiluminescence reagent and anti-mouse horseradish peroxidase (HRP)-conjugated whole antibody (from sheep) were from GE Healthcare UK Ltd. (Buckinghamshire, U.K.). Complete protease inhibitor cocktail was from Roche Diagnostics (Indianapolis, IN). Sulfo-NHS-SS-biotin and streptavidin agarose were from Pierce (Rockford, IL). The mMessage mMachine T7 kit was from Ambion (Austin, TX).

Molecular Biology. A plasmid with the wild-type AE1 sequence in pcDNA3.1(−) was constructed from pJRC9 (*33*). A 603 bp oligonucleotide segment was amplified from pJRC9 by polymerase chain reaction (PCR) with the forward primer 5′-GCG CCA TAT GCT CGA GCA ACT GGA CAC TCA GGA CCA C-3′ and the reverse primer 5′-GCG CGA GCA GAG GCT GTG AAG GAT-3′ to introduce NdeI and XhoI sites at the 5′ end of the AE1 sequence. The PCR product was cloned back into pJRC9 using NdeI and BssHII restriction sites to generate pDEJ3. The AE1 coding sequence from pDEJ3 was introduced into pcDNA3.1(−) within XhoI and HindIII sites to generate pDEJ4.

From this plasmid (pDEJ4), two different constructs were derived. In the first construct, the start codon of AE1 was mutated to a BspEI site (pAB1) by megaprimer mutagenesis (*35*). The first round of PCR with pDEJ4 used the forward primer 5′-CCA CTG CTT ACT GGC TTA TCG-3′ and the reverse mutagenic primer 5′-AGC TCC TCT CCG GAG TGG TCC TG-3′. In the second round of amplification, the product from the first PCR was used as the forward megaprimer and 5′-CGG AAC ACC CTC TCT GAC ATG-3′ as the reverse primer. The second round PCR product was cloned back into pDEJ4 using XhoI and ClaI restriction sites to create pAB1. In the second construct (pAB2), the stop codon of AE1 was mutated to a BspEI site using a similar mutagenesis strategy. In the first round of PCR, the forward primer was 5′-GAT CCA GGA GGT CAA AGA GCA G-3′ and the mutational reverse primer was 5′-GGA CCC GCT CCG GAC ACA GGC-3′. The PCR product was used as a forward megaprimer, and the reverse primer for second round of PCR was 5′-CCA CAG ATG GCT GGC AAC TAG-3′. An ∼3 kb DNA fragment generated by double digestion of pAB2 with XhoI and BspEI was ligated in place of the XhoI-BspEI fragment of pAB1 to generate construct pABCON1, which encoded a concatamer of AE1 (AE1·AE1), where two wild-type AE1 sequences were joined in tandem, connected by a two-residue linker (Ser-Gly).

The AE1 sequence, in which all of the cysteine codons were mutated to serine codons from pJRC26 (*14*), was cloned in place of wild-type AE1 cDNA in pcDNA3, pAE1.WT (a kind gift from R. Reithmeier, University of Toronto, Toronto, ON), to create pHJS4, cysteine-less AE1 in pcDNA3. Plasmids containing a cysteine-less AE1 sequence with the start codon and stop codon mutated to BspEI sites (pAB3 and pAB4, respectively) were constructed by megaprimer mutagenesis, using the same methods and primers described above. An ∼3 kb DNA fragment, generated by double digestion of pAB4 with XhoI and BspEI, was ligated in place of the XhoI-BspEI fragment of pAB3 to create pABCON2, containing the sequence of the cysteine-less concatamer (AE1·AE1-C$^-$).

A cysteine mutation at the Q434 position of AE1 in pAB4 was introduced using the mutagenic reverse primer 5′-CAC TCC

CAT ACA GTT CCG GGT CTT TTC-3′ to generate pAB4-434. The forward primer for the first round of PCR and the reverse primer for the second PCR were 5′-TTG TGT TGC TGG GAC CTG AG-3′ and 5′-ACC AAC ACC ACC AGC AGG AT-3′, respectively. A concatameric plasmid, pCON434X, containing a cysteine codon at the Q434 position of the 5′ (left) subunit of AE1·AE1 [AE1(Q434C)·AE1-C$^-$], was constructed from pAB4-434 and pAB3. To introduce a cysteine codon at the 3′ (right) subunit of AE1·AE1, a plasmid construct, pAB3-434, was generated by introduction of a cysteine codon at the Q434 position of AE1 in pAB3, by megaprimer mutagenesis. Primers used were the same as stated above. Two plasmids, pCONX434 and pCON434-434, containing DNA sequences for concatamers AE1·AE1-(Q434C)-C$^-$ and AE1(Q434C)·AE1(Q434C)-C$^-$, respectively, were constructed from pAB3-434/pAB4 and pAB3-434/pAB4-434 pairs as stated above. The concatameric constructs were subcloned into the *X. laevis* oocyte expression vector, pGEMHE, within SmaI and HindIII sites.

AE1-Ct is a GST fusion protein, which contains the last 40 amino acids of AE1 (residues 872−911). The coding sequence for these amino acids was amplified from pJRC9 (*33*) using the forward primer 5′-CGC GGA TCC GTC CTG CTG CCG CTC ATC TTC-3′ and the reverse primer 5′-CGC GGA TCC TCA CAC AGG CAT GGC CAC TTC GT-3′. The PCR product was inserted into pGEX-6p-1 (GE Healthcare Life Sciences), a GST expression vector, by BamHI digestion and subsequent ligation to generate expression construct pHJC1 (*36*).

DNA sequences generated by PCR were confirmed by DNA sequencing (DNA Core Services Laboratory, Department of Biochemistry, University of Alberta).

Tissue Culture. HEK293 cells were transiently transfected with cDNA by the calcium phosphate method (*37*). Cells were grown in Dulbecco's modified Eagle's medium, supplemented with 5% fetal bovine serum and 5% calf serum at 37 °C in an environment of air, containing 5% CO_2. Cells were used for experiments ~48 h post-transfection.

Determination of Subunit Stoichiometry by Perfluorooctanoic Acid−Polyacrylamide Gel Electrophoresis (PFO−PAGE). The oligomeric states of AE1-C$^-$ and AE1·AE1-C$^-$ were determined, using the PFO−PAGE method, as described previously (*38*), with modifications. Cells were rinsed twice with ice-cold phosphate-buffered saline (PBS) [137 mM NaCl, 2.7 mM KCl, 10 mM Na_2HPO_4, and 1.76 mM KH_2PO_4 (pH 7.4)] and harvested via centrifugation. Cell pellets were resuspended in 4 °C in PBS, containing 1% (v/v) Igepal CA-630 and protease inhibitor cocktail. Proteins were solubilized for 20 min at 4 °C and centrifuged at 16000*g* for 15 min to remove debris. Lysates were mixed in a 1:1 ratio with PFO−PAGE sample buffer [20% (v/v) glycerol, 0.005% bromophenol blue, and 100 mM Tris (pH 8.0)] containing varying concentrations of PFO [from 0 to 8% (w/v)]. Dithiothreitol (DTT) was added to a final concentration of 25 mM. Samples were incubated at 4 °C for 15 min before being loaded onto detergent-free 6% Tris-glycine gels and electrophoresed at 100 V in precooled running buffer [192 mM glycine, 0.5% Na-PFO, and 25 mM Tris (pH 8.5)] at 4 °C. Proteins were immunoblotted as described below.

Immunoblot Analysis. Total membrane preparations from oocytes or HEK293 cell lysates were treated with SDS−PAGE sample loading buffer [10% (v/v) glycerol, 1% (v/v) β-mercaptoethanol, 2% (w/v) SDS, 0.005% (w/v) bromophenol blue, and 65 mM Tris-HCl (pH 6.8)], electrophoresed on 6% polyacrylamide gels (*39*), and transferred onto PVDF membranes. Membranes were incubated in 10 mL of TBST-M {TBST [137 mM NaCl, 0.1% (v/v) Tween 20, and 20 mM Tris base (pH 7.5)] containing 5% (w/v) nonfat dry milk powder} and a 1:2000 monoclonal anti-AE1 antibody dilution, IVF12, kindly provided by M. Jennings (University of Arkansas, Fayetteville, AR) (*40*) for 16 h at 4 °C. Blots were washed three times in TBST and then incubated in TBST-M containing 1:3000 anti-mouse HRP-conjugated antibody dilution, for 1 h at room temperature. After three washes with TBST, blots were visualized using ECL reagent as previously described (*41*) in a Kodak Image Station 440CF. Quantitative densitometric analyses were completed with Kodak Molecular Imaging Software version 4.0.3 (Kodak, Rochester, NY).

Purification of AE1-Ct. BL21-CodonPlus *Escherichia coli* cells were transformed with pHJC1. Transformed cells were grown in LB medium, containing 0.1 mg/mL ampicillin, up to an A_{600} of 0.6−0.8 at 37 °C while being shaken. Isopropyl β-D-1-thiogalactopyranoside was added, to a final concentration of 1 mM, to induce protein expression, and cells were grown for an additional 3 h at 37 °C. Bacterial cells were harvested by centrifugation at 7500*g* for 10 min at 4 °C and were resuspended in 4 °C PBS, containing complete protease inhibitor cocktail. Cells were disrupted by sonication (four times for 60 s) using a W185 probe sonifier (Heat systems-Ultrasonic Inc., Plainview, NY). Triton X-100 was added to a final concentration of 1% (v/v), and the cell suspension was stirred slowly for 30 min. Solubilized cells were centrifuged at 2000*g* for 10 min at 4 °C to remove debris. The supernatant was incubated with 1.2 mL of GSH-Sepharose 4B at room temperature with rotation for 1−2 h to bind the GST-tagged AE1-Ct. After the resin had been washed six times with PBS, AE1-Ct was eluted with three aliquots of 100 μL of glutathione elution buffer [10 mM reduced glutathione and 50 mM Tris-HCl (pH 8.0)]. Protein concentrations were determined by a Bradford protein assay (*42*), and the purity of AE1-Ct was assessed by Coomassie blue-stained SDS−PAGE.

Oocyte Isolation and Injection. Oocytes were obtained from *X. laevis* and isolated as described previously (*43*). Briefly, freshly removed oocytes were incubated for 2 h in modified Barth's medium (MBM) [88 mM NaCl, 1 mM KCl, 2.4 mM $NaHCO_3$, 0.82 mM $MgSO_4$, 0.33 mM $NaNO_3$, 0.41 mM $CaCl_2$, 2.5 mM $C_3H_3O_3Na$, 10 mM HEPES (pH 7.5)], containing 100 mg/L penicillin, 50 mg/L gentamycin sulfate, and 2 mg/mL collagenase type I, with agitation. Defolliculated oocytes at stages V and VI (prophase-arrested) were selected and maintained at 18 °C in MBM. For AE1 protein expression in *X. laevis* oocytes, cRNA was synthesized using the mMessage mMachine T7 kit from cDNAs cloned into the pGEMHE vector. cRNA integrity was verified by agarose gel electrophoresis, and the concentration was determined by spectrophotometry. Oocytes were injected with 50 nL of 1.5 ng/nL cRNA or 50 nL of water and incubated in MBM at 18 °C for 4 days.

Isolation of X. laevis Oocyte Membranes. To isolate membranes, oocytes were treated as described previously (*44*). Briefly, 4 days postinjection, oocytes were homogenized by being pipetted up and down in MBM containing protease inhibitor cocktail and centrifuged at 250 *g* for 10 min at 4 °C. The supernatant was collected and centrifuged at 13000*g* for 30 min at 4 °C. The membrane pellet was resuspended in MBM (2 μL/oocyte) and frozen at −20 °C until it was used.

Cl^-/HCO_3^- Exchange Assays. HEK293 cells were grown on poly-L-lysine-coated coverslips in 60 mm dishes. Cells were transiently transfected with AE1 or AE1·AE1, as described above.

Anion exchange assays were performed as described previously (*34*). Briefly, 2 days post-transfection, coverslips were rinsed three times in serum-free Dulbecco's modified Eagle's medium (DMEM) and incubated in serum-free DMEM, containing 2 μM BCECF-AM, at 37 °C for 15 min. Coverslips were mounted in a cuvette and alternately perfused (3.5 mL/min) at 20 °C with Ringer's buffer [5 mM glucose, 5 mM potassium gluconate, 1 mM calcium gluconate, 1 mM $MgSO_4$, 2.5 mM NaH_2PO_4, 25 mM $NaHCO_3$, and 10 mM HEPES (pH 7.4)], containing either 140 mM NaCl or 140 mM sodium gluconate. Both buffers were continuously bubbled with air, containing 5% CO_2. Fluorescence changes were monitored in a Photon Technologies International (London, ON) RCR fluorimeter at excitation wavelengths of 440 and 503 nm, and the emission wavelength 529 nm. Fluorescence data were converted to intracellular pH (pH_i) by calibration using the nigericin/high-potassium method (*45*). Initial rates of pH_i change were monitored by linear regression measured using Felix (Photon Technologies International) to provide a measure of anion exchange activity. Transport activity was normalized to the expression of AE1 or AE1·AE1, as quantified on immunoblots of cell lysates prepared from the cells used in transport assays.

Cell Surface Biotinylation Assay. Cell surface processing assays were preformed essentially as described previously (*46*). HEK293 cells were transiently transfected with cDNA encoding AE1 and AE1·AE1. Forty-eight hours post-transfection, cells were rinsed sequentially with 4 °C PBS and borate buffer [154 mM NaCl, 7.2 mM KCl, 1.8 mM $CaCl_2$, and 10 mM boric acid (pH 9.0)] and incubated for 30 min at 4 °C in borate buffer, containing sulfo-NHS-SS-biotin (0.5 mg/mL) (Pierce). Cells were washed with quenching buffer [192 mM glycine and 25 mM Tris (pH 8.3)] and solubilized for 20 min on ice in IPB [1% (v/v) Igepal CA-630, 0.5% (w/v) deoxycholic acid, 150 mM NaCl, 5 mM EDTA, and 10 mM Tris-HCl (pH 7.5)], containing complete protease inhibitor. Cell lysates were centrifuged for 20 min at 13200*g* and 4 °C, and the pellet was discarded. For each solubilized sample, half of the supernatant was retained for further analysis (total protein, *T*). The remaining half was incubated with 50 μL of streptavidin agarose resin for 16 h at 4 °C with gentle rotation. The supernatant was collected after centrifugation for 2 min at 8000*g* (unbound protein, *U*). Both *T* and *U* fractions of each sample were treated with SDS−PAGE sample buffer and separated via a 6% acrylamide SDS−PAGE gel. AE1 was detected on immunoblots with the anti-AE1 antibody, IVF12, and quantified by densitometry as described above. The percentage of biotinylated protein was calculated as $[(T - U)/T] \times 100\%$, which represents the fraction of protein processed to the cell surface.

Whole Mount Oocyte Immunochemistry. After removal of the follicle membranes, oocytes were injected with water or cRNA as described above and incubated at 18 °C for 4 days. Oocytes were fixed in 3% paraformaldehyde in PBS for 15 min. Oocytes were washed three times in PBS, containing 50 mM NH_4Cl, and permeabilized with 0.1% Triton X-100 in PBS for 4 min. Oocytes were then washed three times for 5 min in PBS and blocked for 30 min in 2% BSA in PBS. Next oocytes were incubated in PBS, containing 2% BSA and monoclonal anti-AE1 antibody, IVF12 (1:2000), for 1 h at 20 °C, followed by three washes with PBS for 10 min. Oocytes were incubated for 30 min in secondary antibody, Alexa Fluor 488-tagged chicken anti-mouse IgG (1:200) in PBS containing 2% BSA. After three 10 min washes in PBS, oocytes were mounted in Vectashield (Vector Laboratories, Burlingame, CA). Images were taken using the confocal microscopy parameters described below.

Confocal Microscopy. For confocal microscopic images, oocytes were immunostained and fixed as described above. Images were acquired on a spinning-disk microscope (WaveFx from Quorum Technologies, Guelph, ON) set up on an Olympus IX-81 inverted stand (Olympus, Markham, ON). Alexa Fluor 488 was excited at 491 nm. Images were acquired through a 10× objective (N.A. 0.3) with an EMCCD camera (Hamamatsu, Tokyo, Japan). Z slices were acquired through the oocytes, and two-dimensional (2D) or three-dimensional (3D) images were produced using Volocity (Improvision/Perkin-Elmer).

To examine the fluorescence of oocytes treated with fluorescent compounds, 3 days postinjection with cRNA, oocytes were incubated with 10 mM 3-maleimidopropionic acid in MBM for 1 h at 18 °C to block the endogenous reactive sulfhydryl groups in the oocyte membrane (*47*). Oocytes were washed three times in MBM and incubated at 18 °C for an additional day. On the fourth day postinjection, oocytes were incubated for 20 min in MBM, containing 270 μM AF. After three washes with MBM, oocytes were mounted with Vectashield as described above. Another group of oocytes was mounted similarly after sequential incubation with MBM containing 270 μM AF and then with MBM containing 1.5 μM $DiIC_{12}(3)$. Bound AF was excited by a 491 nm laser line (Spectral Applied Research, Richmond Hill, ON) to acquire images.

Fluorescence Spectroscopy. Endogenous reactive sulfhydryl groups in the oocyte membrane were blocked as described above. Individual oocytes, expressing AE1(Q434C)·AE1-C^-, were labeled with fluorescence probes by incubation with MBM, containing either 270 μM AF, 350 μM TMR-MTS, or 1.5 μM $DiIC_{12}(3)$ at 20 °C in the dark, over a range of incubation periods (from 0 to 25 min) to determine the labeling kinetics. For intersubunit fluorescence labeling, oocytes were sequentially labeled in the dark with MBM containing 270 μM AF (donor), up to 20% of the maximum labeling, and MBM containing 350 μM TMR-MTS (acceptor), to saturation. To label AE1·AE1 with donor, and the membrane with an acceptor, we sequentially labeled oocytes in the dark with MBM containing 270 μM AF (donor) or MBM containing 1.5 μM $DiIC_{12}(3)$ (acceptor), both up to saturation. Under all conditions, the unbound fluorophore was removed with three washes in 10 mL of MBM prior to fluorescence measurements. Labeled oocytes were placed in a custom-designed oocyte holder (*48*) and inserted into a standard 1 cm × 1 cm polystyrene cuvette, and fluorescence spectra were recorded on a PTI fluorimeter (Photon Technologies International).

To determine the kinetics of labeling with AF and TMR-MTS, oocytes expressing AE1(Q434C)·AE1-C^- labeled with either AF, TMR-MTS, or $DiIC_{12}(3)$ were directly excited at 484, 500, or 505 nm, respectively, to record the whole emission spectra. The AF emission spectrum overlaps with the TMR-MTS and $DiIC_{12}(3)$ excitation spectra and therefore could serve as an energy transfer donor (D) for both acceptors (A).

For donor and acceptor fluorophore-labeled AE1(Q434C)·AE1(Q434C)-C^-, the strategy was based on probability calculations, as shown previously (*49*). Briefly, each cysteine residue in the double-cysteine mutant can be labeled with D or A leading to three possibilities: 4% D:D, which contributes to fluorescence but not to FRET; 32% D:A, which contributes to both fluorescence and energy transfer; and 64% A:A, which has negligible fluorescence at the donor excitation wavelength and does not contribute to FRET. We estimate that ~10% of the donor fluorescence is derived from two donors and will

not transfer energy. We therefore corrected our distance calculations on this value.

To monitor energy transfer, we excited AF at 475 nm, a wavelength that is below the maximum excitation wavelength of this fluorophore, to prevent direct excitation of acceptor fluorophores, TMR-MTS or $DiIC_{12}(3)$. Fluorescence spectra were recorded over the range of 500−700 nm. The AF fluorescence intensity of oocytes expressing AE1(Q434C)·AE1-C$^-$, AE1·AE1(Q434C)-C$^-$, or AE1(Q434C)·AE1(Q434C)-C$^-$ was corrected by the autofluorescence measured from a single oocyte expressing AE1·AE1-C$^-$ and labeled with AF.

Spectra from four to five oocytes, labeled with AF as described above, were averaged. The AF fluorescence was detected with an excitation wavelength of 475 nm. The same oocyte was then incubated in MBM, containing the acceptor probe, $DiIC_{12}(3)$ or TMR-MTS, and washed in MBM three times to remove unbound fluorophores. AF fluorescence was recorded again. AF spectrum quenching (*50*) in the presence of the acceptor, TMR-MTS or $DiIC_{12}(3)$, was used to assess FRET. The decrease in fluorescence at 520 nm was measured, as at this wavelength both autofluorescence and acceptor fluorescence were negligible with excitation at 475 nm.

Distance Calculations by Fluorescence Resonance Energy Transfer. FRET is a distance-dependent interaction between electronically excited states of two molecules, in which energy is transferred from an excited donor fluorophore to an acceptor fluorophore. The efficiency of energy transferred (E) is defined as

$$E = 1 - F/F_0 \quad (1)$$

where F and F_0 are the donor fluorescence intensities in the presence and absence of the acceptor, respectively. The efficiency of energy transfer depends on the distance (R) between the donor and acceptor according to

$$E = 1/[1 + (R/R_0)^6] \quad (2)$$

where R_0 (Förster distance) is the distance at which half of the energy is transferred. R_0 is calculated as follows:

$$R_0^6 = [9Q_D(\ln 10)K^2J]/(128\pi^5 n^4 N_A) \quad (3)$$

where Q_D is the quantum yield of the donor in the absence of the acceptor, K^2 is the dipole orientation factor (usually assumed to be $^2/_3$ when the donor and acceptor are mobile), n is the refractive index of the medium, N_A is Avogadro's number, and J is the spectral overlap integral. Here we assumed the refractive index of biomolecules in aqueous solution to be 1.4 (*51*). The spectral overlap integral, J, is calculated by

$$J = \int f_0(\lambda)\varepsilon_A(\lambda)\lambda^4 \, d\lambda \quad (4)$$

where f_0 is the normalized donor emission spectrum and ε_A is the acceptor molar extinction coefficient. Our R_0 value of ~50 Å agrees with the previously published value of the AF/TMR-MTS FRET couple (*52*).

Anisotropy Measurements. Uncertainties in K^2 can lead to error in the estimated R_0. We therefore measured anisotropy from a single oocyte labeled with AF (r_d) or TMR-MTS (r_a). We used a polarized cube beam splitter to measure the parallel and perpendicular emitted light at the same time and used eq 5 for the calculation of anisotropy (r).

$$r = (I_\parallel - I_\perp)/(I_\parallel + 2I_\perp) \quad (5)$$

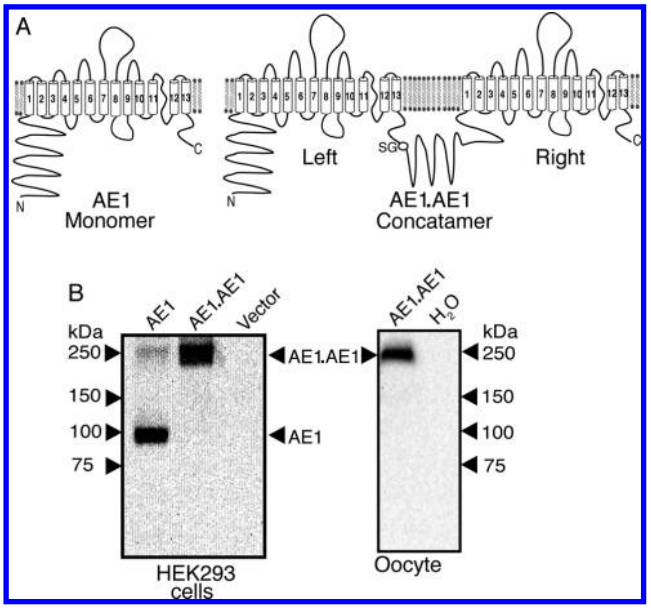

FIGURE 1: Expression of AE1·AE1 in HEK293 cells and *X. laevis* oocytes. (A) Schematic diagram of AE1 and AE1·AE1. Human AE1 monomers joined in tandem with a two-residue (serine and glycine) linker and expressed as a single ~200 kDa polypeptide. Left and right labels differentiate the N- and C-terminal AE1 subunits within the concatamer, respectively. The circled region, labeled SG, indicates the site at which a two-residue Ser-Gly linker was introduced between the two AE1 subunits. (B) HEK293 cells were transfected with cDNA encoding WT AE1, AE1·AE1 concatamer, or empty vector. *X. laevis* oocytes were injected with AE1·AE1 cRNA or water (H_2O), and membranes were isolated. Whole cell lysates of HEK293 cells or solubilized *X. laevis* membranes from 10 oocytes were resolved on 6% acrylamide SDS−PAGE gels and transferred to PVDF membranes. Immunoblots were probed with IVF12 anti-AE1 monoclonal antibody.

where $I_\parallel$ is the parallel and $I_\perp$ the perpendicular emitted light with respect to the polarized excitation light. The parallel and perpendicular emitted light were measured in a Photon Technologies International RCR fluorimeter with polarized filters (motorized, computer-controlled Glan-Thompson polarizers, K-141-B, Photon Technologies International). The anisotropy values obtained for the donor (r_d) and acceptor (r_a) were used to set the upper and lower limits for K^2 as shown in eqs 6 and 7.

$$K_{max}^2 = 2/3(1 + Fr_d + Fr_a + 3Fr_dFr_a) \quad (6)$$

$$K_{min}^2 = 2/3[1 - (Fr_d + Fr_a)/2] \quad (7)$$

Fr_d and Fr_a are described in eqs 8 and 9, respectively, and r_0 is the fundemental anisotropy of each fluorophore (0.4 for AF and 0.4 for TMR-MTS):

$$Fr_d = (r_d/r_0)^{0.5} \quad (8)$$

$$Fr_a = (r_a/r_0)^{0.5} \quad (9)$$

Statistical Analysis. Statistical analyses were performed using Prism (GraphPad Software Inc.). Groups were compared by a paired t test, or ANOVA, where $P < 0.05$ was considered significant.

RESULTS

Construction and Expression of the AE1 Concatamer. Concatameric AE1 (AE1·AE1) was constructed by fusing the coding sequences for two human AE1 monomers consecutively,

connected by a short serine-glycine linker (Figure 1A). AE1·AE1 allows the mutagenesis of any combination of amino acids within an entire AE1 dimer, the fundamental unit of AE1 (*6*). HEK293 cells were transfected with cDNA of AE1 or AE1·AE1, while cRNA encoding AE1, AE1·AE1, or a water control was injected into *X. laevis* oocytes. Expression of the AE1 monomer and concatamer was confirmed by immunoblot analysis (Figure 1B). Immunoreactive bands were detected with the anti-AE1 antibody at approximately 100 kDa for the monomer, AE1, and approximately 200 kDa for the concatamer, AE1·AE1 (Figure 1B). No AE1 band was detected from vector-transfected HEK293 cells or water-injected oocytes by the monoclonal antibody indicating specificity of immunodetection. A faint band, consistent with dimeric AE1 that was not dissociated by SDS, was observed for HEK293 cells transfected with monomeric AE1 cDNA, indicating that AE1 dimers were not fully dissociated during electrophoresis. These experiments indicate that AE1·AE1 is expressed at a level similar to that of AE1 in HEK293 cells as determined by densitometry.

To determine the number of molecules of AE1·AE1 expressed in a single oocyte, solubilized oocyte membranes, expressing AE1·AE1, were immunoblotted and compared to a known amount of AE1-Ct, run in parallel. AE1-Ct is a glutathione *S*-transferase fusion protein fused to the 40 C-terminal amino acids of human AE1. Because the anti-AE1 antibody, IVF12, recognizes the C-terminus of AE1, blots loaded with AE1-Ct allowed measurements of AE1·AE1 expression following densitometry of the immunoblots. This analysis revealed that each oocyte expresses an amount of AE1 C-terminal epitopes equivalent to 3.9 ng of AE1 monomer, corresponding to 1.2×10^{10} AE1·AE1 molecules per oocyte (data not shown), which is in line with expression levels of other transporters whose cRNA has been expressed in this system (*53*, *54*).

Cell Surface Expression of AE1·AE1. Small changes in protein structure can affect the way a membrane protein is processed through the biosynthetic pathway to the plasma membrane (*55*). We therefore assessed the degree of plasma membrane processing of AE1·AE1 and AE1·AE1-C$^-$, a version of the concatamer in which all cysteine residues were mutated to serine residues. AE1·AE1-C$^-$ was prepared using a cysteine-less AE1 (AE1-C$^-$) mutant previously characterized as functional (*33*). Intact HEK293 cells expressing AE1, AE1·AE1, and AE1·AE1-C$^-$ were incubated with the membrane impermeant, amine-directed compound sulfo-NHS-SS-biotin, which labels primary amine groups at the extracellular surface of the plasma membrane. Detergent lysates were prepared from the cells, and biotinylated proteins were removed by incubation with streptavidin resin. The total lysate (total) and the fraction that did not bind streptavidin resin (unbound) were analyzed on immunoblots probed with anti-AE1 antibody, IVF12 (Figure 2A). AE1, AE1·AE1, and AE1·AE1-C$^-$ were processed to the plasma membrane with efficiencies of 40 ± 1, 35 ± 2, and 34 ± 1%, respectively (Figure 2B). Three-way ANOVA revealed that the difference was not statistically significant ($P > 0.05$).

Localization of AE1 and AE1·AE1 at the plasma membrane of *X. laevis* oocytes was assessed by the immunochemistry of oocytes treated with the respective cRNAs and compared to that of oocytes treated with water. Oocytes were permeabilized with 0.1% Triton X-100, incubated with anti-AE1 antibody, IVF12, and further incubated with a secondary fluorescent antibody, Alexa Fluor 488-conjugated chicken anti-mouse antibody. Confocal immunofluorescence microscopy revealed both wild-type and concatameric proteins as plasma membrane-localized at qualitatively similar levels (Figure 2C). The water-treated control oocytes exhibited no immunoreactivity, indicating specificity of detection (Figure 2C).

Cl^-/HCO_3^- Exchange Activity of AE1·AE1. Cl^-/HCO_3^- exchange assays were performed to study AE1·AE1 function in transiently transfected HEK293 cells (Figure 3). In these assays, a pH sensitive fluorescent probe, BCECF-AM, was used to report on the cytosolic pH changes associated with the Cl^-/HCO_3^- exchange activity of AE1- or AE1·AE1-transfected HEK293 cells grown on glass coverslips. Initially, cells were perfused with chloride-containing Ringer's buffer. When the cells were perfused with chloride-free Ringer's buffer, AE1 mediates efflux of chloride in exchange for bicarbonate, which alkalinizes the cell (Figure 3A). Initial rates of cytosolic alkalinization were determined for HEK293 cells transfected with AE1 or AE1·AE1 and normalized to the amount of AE1 present at the plasma membrane (Figure 3B). Cl^-/HCO_3^- exchange activities of AE1 and AE1·AE1 (per AE1 unit) were statistically indistinguishable. This indicated that the linkage of two AE1 units in tandem did not affect the functional activity of each AE1 subunit as an anion exchanger.

Oligomeric State of the Concatamer. One objective of this study was to design an AE1 concatamer suitable for FRET studies. AE1 exists in the erythrocyte membrane as a mixture of dimers and tetramers, with tetramers forming by dimerization of dimers, upon association with the cytoskeleton (*6*). If AE1·AE1 dimerizes, then FRET between the individual concatamers would impair the ability to interpret FRET data.

The density of AE1·AE1 on the oocyte cell surface was determined to examine the possibility of FRET between two adjacent concatamers. The oocyte surface area (SA) was calculated from the surface area equation of a sphere ($SA = 4\pi r^2$, where r is the oocyte radius, which ranges from 0.5 to 0.6 mm), implying a surface area of $3.0-4.5 \times 10^6$ μm^2. Quantification of AE1·AE1 revealed that 1.2×10^{10} AE1·AE1 units are expressed in each oocyte. Assuming that all AE1·AE1 molecules are processed to the plasma membrane, a density of $2.2-3.3 \times 10^3$ molecules/μm^2 is expected. In this range of AE1·AE1 densities, the distance between two concatamer molecules should be 195−286 Å, a distance over which FRET is not possible, unless the concatamer forms higher-order oligomers.

We assessed the oligomeric state of the AE1 concatamer by two different methods. First, the oligomeric states of AE1·AE1-C$^-$ and AE1-C$^-$, expressed in HEK293 cells, were determined by PFO−PAGE (Figure 4). PFO−PAGE is an electrophoretic approach that uses the molecule perfluorooctanoic acid (PFO) as a relatively nondenaturing detergent to resolve proteins, while maintaining protein−protein interactions. A gradient of PFO concentrations in the sample buffer was used to either maintain (low concentrations) or disrupt (high concentrations) any oligomeric complexes. The oligomeric state of AE1-C$^-$ was used as a positive control, because AE1 is known to form dimers (*56*). Consistent with this, PFO−PAGE resolved AE1-C$^-$ into two bands with molecular masses of approximately 200 and 100 kDa, representing dimeric and monomeric states of the protein, respectively. With increasing concentrations of PFO in the sample buffer, a greater fraction of monomeric AE1-C$^-$ was detected. In contrast, AE1·AE1-C$^-$ appeared as a single band of approximately 200 kDa at all PFO concentrations, consistent with AE1·AE1 monomers. No higher-molecular mass species

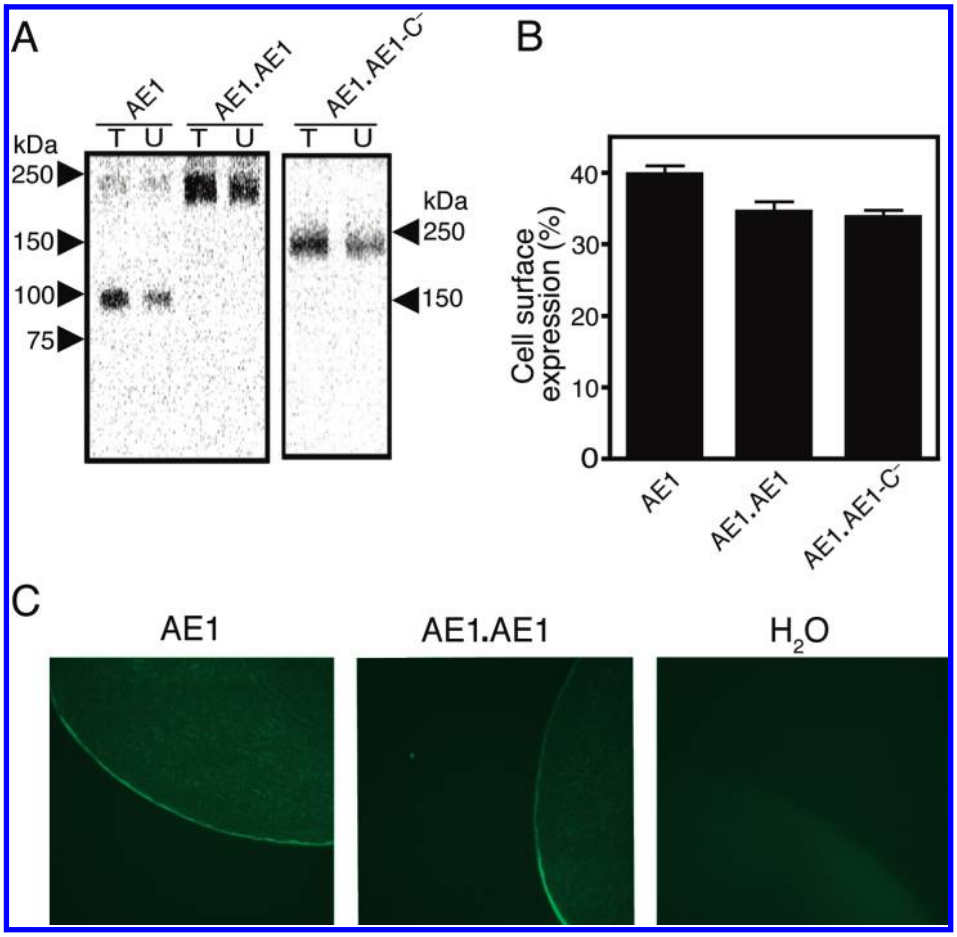

FIGURE 2: Cell surface expression of AE1, AE1·AE1, and AE1·AE1-C$^-$. (A) Cell surface expression levels of AE1, AE1·AE1, and AE1·AE1-C$^-$ were determined by cell surface biotinylation. HEK293 cells were incubated with sulfo-NHS-SS-biotin, a membrane impermeant, amine-directed compound, 48 h post-transfection. Cells were solubilized, and half of the sample protein was incubated with streptavidin Sepharose to remove biotinylated protein. Total (T) and unbound (U) proteins were detected on immunoblots with anti-AE1 antibody, IVF12. (B) Quantification of cell surface expression by densitometry. Cell surface protein (biotinylated fraction) was calculated as $[(T - U)/T] \times 100\%$. Statistical analysis was done by ANOVA ($P > 0.05$). The standard error is shown with error bars ($n = 4$). (C) *X. laevis* oocytes were treated with 75 ng of cRNA encoding AE1, AE1·AE1, or an equal volume of H_2O, as indicated. Four days postinjection, intact cells were subjected to immunocytochemistry, and AE1 was detected by incubation with IVF12, the mouse monoclonal anti-AE1 antibody, followed by the Alexa Fluor 488-conjugated chicken anti-mouse antibody.

was identified for AE1·AE1-C$^-$, suggestingthat the AE1 concatamer does not associate into oligomers.

We used FRET as a second approach to examine the AE1·AE1 oligomeric state in *X. laevis* oocytes. If AE1 concatamers associate, the transfer of energy between fluorophores on different concatameric units will be possible. To set the stage for FRET experiments, labeling kinetics and spectral properties of fluorescently labeled AE1(Q434C)·AE1-C$^-$ expressed in oocytes were determined. AE1(Q434C)·AE1-C$^-$ corresponds to the AE1 concatamer with no cysteine residues, except at Q434 of the left subunit (Figure 5A). The Q434C mutation is located in extracellular (EC) loop 1 of AE1 (*2*), making it accessible with the cysteine-reactive fluorescent compounds AF and TMR-MTS. To suppress the background fluorescence of oocytes, resulting from endogenous cysteine-containing proteins, oocytes were treated with 3-maleimidopropionic 3 days after being treated with cRNA, an approach used previously in studies using cysteine-directed fluorescent probes in oocytes (*57*). The kinetics of labeling of AE1(Q434C)·AE1-C$^-$ by AF and TMR-MTS were measured to determine the appropriate labeling conditions to achieve 20% saturation, by monitoring fluorescence as a function of incubation time (Figure 5B,C). One of the primary conditions required for FRET to occur is the overlap of the donor (AF) emission spectrum with the acceptor (TMR-MTS) excitation spectrum. The emission spectrum of AF (donor) and the excitation spectrum of TMR-MTS (acceptor) (Figure 5D) were used to calculate the overlap integral. The calculated overlap integral (1.3×10^{-13} M^{-1} cm^3) (eq 4) is relatively high in comparison to those of many other donor−acceptor pairs (*51*), resulting in an R_0 of ~50 Å (eq 3). This high emission/excitation overlap makes the AF/TMR-MTS pair suitable for FRET studies in the distance range of 50 Å.

In experiments that aim to assess the AE1·AE1 oligomeric state by FRET, AE1·AE1-C$^-$, AE1(Q434C)·AE1-C$^-$, and AE1·AE1(Q434C)-C$^-$ were expressed individually by cRNA injection in oocytes (Figure 6). In another set of oocytes, AE1(Q434C)·AE1-C$^-$ and AE1·AE1(Q434C)-C$^-$ were coexpressed. Each group of oocytes was labeled with the donor (D) fluorophore, AF, up to 20% of the maximal labeling. The advantage of labeling up to 20% of the maximal level is that, at this labeling stoichiometry, the probability of two adjacent cysteines being labeled with the donor is low (4%). AF (donor, D) was excited at 475 nm, because at this wavelength the acceptor fluorophore (TMR-MTS) has negligible fluorescence at the donor's wavelength of maximum emission (520 nm) (*52*). As a consequence, TMR fluorescence does not contribute to the fluorescence measured when monitoring the fluorescence of AF. Next, the same oocyte was labeled up to

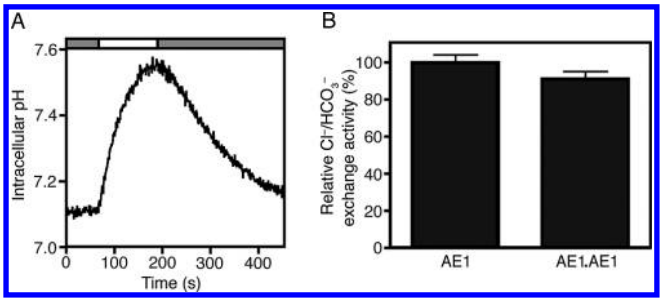

FIGURE 3: Cl^-/HCO_3^- exchange activity of the AE1·AE1 concatamer. (A) HEK293 cells transiently transfected with cDNA encoding AE1·AE1 were grown on glass coverslips. The coverslips were incubated with the pH-sensitive dye BCECF-AM and then mounted in a fluorescence cuvette. The cells were perfused alternatively with chloride-containing Ringer's buffer (gray bar) or chloride-free Ringer's buffer (white bar), and the intracellular pH was monitored. (B) Rates of Cl^-/HCO_3^- exchange were measured from the initial slopes observed after buffer changes (from Cl^--containing to Cl^--free) and converted to relative transport, with the transport rate of AE1 considered to be 100%. The transport rates were normalized to protein expression. A paired *t* test revealed that there was no significant difference between the rates ($p = 0.18$; $n = 4$).

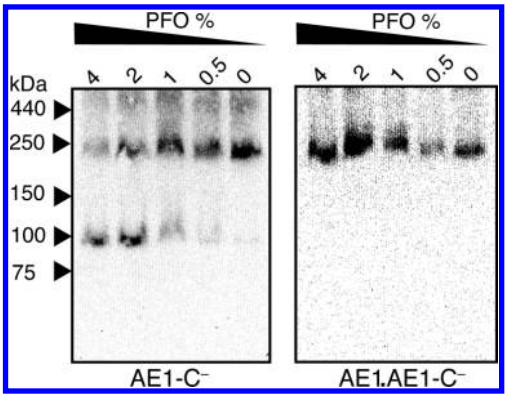

FIGURE 4: AE1·AE1 oligomeric state in HEK293 cells. HEK293 cells were transiently transfected with either AE1-C^- or AE1·AE1-C^- cDNA. Forty-eight hours post-transfection, cell lysates were combined with sample buffer containing different concentrations of PFO (as indicated at the top of each lane) for 15 min at 4 °C. Samples were electrophoresed on 6% acrylamide gels containing no detergent using PFO−PAGE running buffer, containing 0.5% PFO, and transferred to PVDF membranes. Monomeric AE1 and concatameric AE1 were detected with the monoclonal anti-AE1 antibody, IVF12. Prestained protein markers along with ferritin were run in parallel as molecular mass standards. Ferritin (440 kDa) was detected with Ponceau S staining (data not shown).

saturation levels with the acceptor (A) fluorophore TMR-MTS, and the donor fluorescence was measured in the presence of the acceptor. The fluorescence of oocytes expressing AE1·AE1-C^- and labeled with the donor probe AF served as a measurement of background fluorescence, which can be attributed to labeling of endogenous cysteines in the oocyte, as indicated by the dashed line (Figure 6). The background fluorescence (indicated by the dashed line in Figures 6 and 7) was subtracted from all values used for FRET efficiency calculations.

Because each concatamer contains only a single cysteine residue available for labeling, and therefore only a single fluorescent probe, we reasoned that FRET could occur only if concatamers associate. The fluorescence of AE1(Q434C)·AE1-C^- and AE1·AE1(Q434C)-C^-, labeled with donor and acceptor, was monitored to test whether the concatamers might associate in such a way that allows close apposition of Q434C in either the left of right subunit. Similarly, fluorescence studies of the two proteins coexpressed were used to determine whether an antiparallel arrangement might occur, where the Q434C mutation in the left subunit comes close to that in the right. No significant FRET was observed under any of the conditions tested, indicating that AE1·AE1 does not oligomerize in oocytes (Figure 6). The AE1 dimer unit has dimensions of 60 Å × 110 Å (*16*), so if oligomerization of AE1·AE1 occurred, the Q434C position would be within the 100 Å FRET limit in one of these orientations.

Anisotropy Measurements. To calculate the error associated with R_0 estimation, we determined the relative mobility of AF and TMR-MTS, by measuring emitted light from AE1(Q434C)·AE1-C^- labeled with each probe, when excited by polarized light. Low anisotropy values of 0.020 ± 0.003 (r_d) ($n = 6$) and 0.030 ± 0.009 (r_a) ($n = 5$), corresponding to a single cysteine labeled with AF and TMR-MTS, respectively, indicate that the fluorescent probes coupled to Q434C are highly mobile. These values were used to establish the upper and lower orientation factor limits for the R_0 calculation [1.1 (K_{max}^2) and 0.5 (K_{min}^2), respectively] from eqs 6 and 7. The upper and lower limits of the orientation factor were applied to eq 3 to obtain maximum and minimum values for R_0. Thus, we estimated a maximal error of 5 Å in R_0. The calculated orientation factor range, however, allows for the use of the standard k^2 value of $^2/_3$ in our distance estimate (*51*).

Measurement of Distances in AE1·AE1. To assess the distance between two locations in the AE1 units across the dimer interface, we measured FRET in AE1(Q434C)·AE1(Q434C)-C^- (Figure 7A), expressed in *X. laevis* oocytes. AE1(Q434C)·AE1-(Q434C)-C^- was labeled with AF (donor), up to 20% saturation, and to assess the efficiency of energy transfer, its fluorescence was recorded before and after it was labeled with TMR-MTS (acceptor) (Figure 7B). The donor (AF) fluorescence decreased by 46 ± 1% (Figure 7C) upon the addition of acceptor, due to FRET. To calculate the Q434C−Q434C distance, we used the Förster equation (eq 2) by determining the donor fluorescence in the presence (F) and absence (F_0) of the acceptor. A FRET efficiency of 0.54 suggests that the labeled residues are approximately 49 Å from each other. An estimate of the error on this value arises from the error in R_0 (5 Å). Figure 7D represents the scale of the distance between two Q434C residues located at the end of TM2 on the two-dimensional projection map of the AE1 dimer, determined by cryoelectron microscopy (*16*). Finally, FRET observed between labeled Q434C residues in AE1·AE1 can be used as a positive control for the FRET experiments performed to assess the oligomeric state of AE1·AE1 (Figure 6), because it shows that if the distance between the donor and acceptor is < 100 Å it is possible to observe FRET.

Distance from Q434 of AE1-C^- to the Lipid Bilayer. Oocytes expressing AE1(Q434C)·AE1-C^- were labeled with AF fluorescent donor, and the membrane was labeled with the acceptor $DiIC_{12}(3)$ (Figure 8A), a 12-carbon aliphatic chain coupled to a dialkylindocarbocyanine (DiI) fluorescent group (*58*). Residue Q434 is of special interest, because this residue maps to extracellular loop 1 (*2*), close to TM2 at the membrane interface region. The membrane surface proximity of Q434 ensures a relatively fixed distance from the residue to the membrane surface. Because the distribution of fluorescence acceptor molecules is random in the membrane, there is a range of donor−acceptor distances, which is reflected in an averaged FRET efficiency. FRET efficiency depends on the distance between the donor and acceptor, as well as on the acceptor concentration in the membrane (*51*). The labeling kinetics of the donor, AF, coupled to AE1(Q434C)·AE1-C^- (Figure 5B) and the membrane embedding

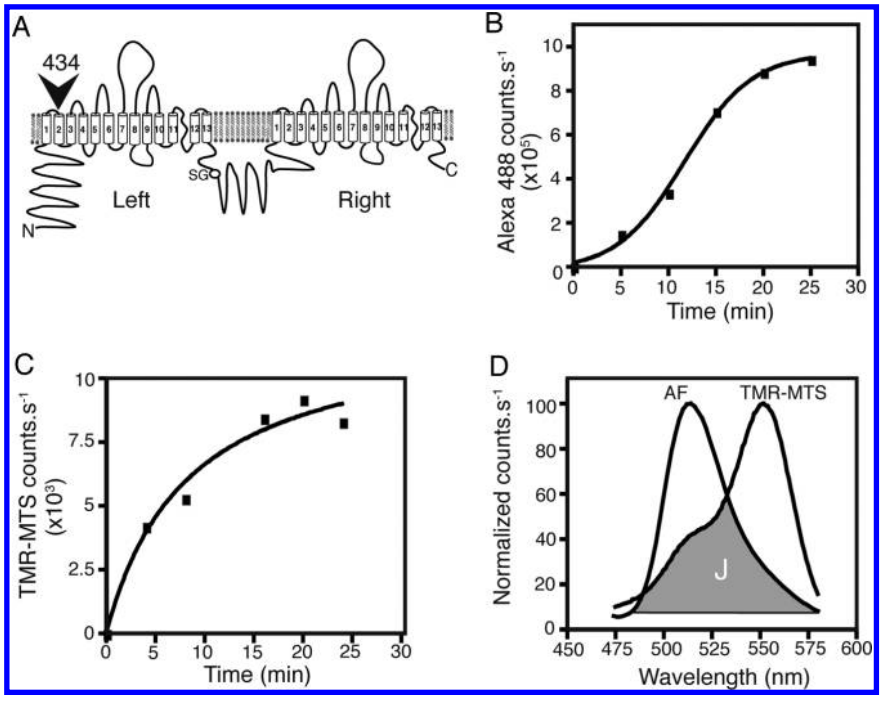

FIGURE 5: Fluorescence labeling of AE1(Q434C)·AE1-C$^-$. (A) A single cysteine was introduced via substitution of Q434 on the left subunit of AE1·AE1-C$^-$ (as indicated by the arrow) to produce AE1(Q434C)·AE1-C$^-$. AE1(Q434C)·AE1-C$^-$ was expressed in oocytes. Three days postinjection, oocytes were treated with 1 mM 3-maleimidopropionic acid to block endogenous cysteines. Oocytes were then incubated for one additional day to allow AE1(Q434C)·AE1-C$^-$ expression at 18 °C. On the fourth day postinjection, oocytes were incubated in MBM, containing 270 μM Alexa Fluor 488 C_5-maleimide (AF) (B) or 350 μM TMR-MTS (C) at 20 °C in the dark for different periods of time. At the indicated time points, the unbound probe was washed away. Individual oocytes labeled with AF were excited with 484 nm light, and the fluorescence was recorded from 500 to 700 nm. The fluorescence observed at the maximal emission wavelength (520 nm) was used for labeling time course evaluation. The results obtained from the labeling of individual oocytes were fitted to a sigmoid function (B). An oocyte labeled with TMR-MTS was excited at 500 nm, and the fluorescence was recorded from 520 to 700 nm. The fluorescence observed at the maximal emission wavelength (575 nm) was used for labeling time course evaluation. The results were fitted with an exponential function (C). (D) Overlap of the Alexa Fluor 488 C_5-maleimide (AF)-labeled oocyte emission spectrum (475 nm excitation) and the TMR-MTS-labeled oocyte excitation spectrum (620 nm emission). The integral of this overlap (*J*) is colored gray.

of the acceptor probe $DiIC_{12}(3)$ (Figure 8B) were established. Emission and excitation spectra were recorded for an individual oocyte labeled with either AF or $DiIC_{12}(3)$. The overlap of donor emission spectra and acceptor excitation spectra indicated that the donor−acceptor couple was suitable for FRET (Figure 8C). The spectral overlap integral (*J*), calculated with eq 4, was used in eq 3 to estimate the Förster distance (R_0) for this pair to be 33 Å. This Förster distance is identical to previously published values for the Alexa Fluor 488 C_5-maleimide (AF) and $DiIC_{18}(3)$ pair (*59*).

The transfer of energy between AF-labeled AE1(Q434C)·AE1-C$^-$ and the $DiIC_{12}(3)$-labeled oocyte membrane was visualized by the quenching of AF donor emission resulting from the transfer of energy to $DiIC_{12}(3)$ using confocal microscopy and quantified (Figure 9). To exclude the possibility that the observed decrease in AF can be attributed to donor fluorophore bleaching or chemical modifications associated with organic reagents used to dissolve the acceptor probe, we treated a group of oocytes similarly, but in the absence of acceptor. In these oocytes, donor fluorescence remained unchanged (data not shown). In addition, subsequent excitations of AF at 460 nm did not have a noticeable effect on the intensity of the donor fluorescence (data not shown). This indicates that the decrease in the fluorescence intensity of AF was caused by the transfer of energy to $DiIC_{12}(3)$. The possibility of errors in the measured energy transfer due to acceptor transbilayer migration ("flip-flop") is not likely at room temperature and in the time frame of the experiment (*60*).

We utilized confocal microscopy to evaluate donor fluorescence in the presence or absence of an acceptor. Oocytes expressing AE1(Q434C)·AE1-C$^-$ were labeled with either AF (donor), $DiIC_{12}(3)$ (acceptor), or both. Labeling treatments maintained the round shape of oocytes, and the fluorophores were distributed homogeneously on the membrane surface (Figure 8D). Donor fluorescence decreased in the presence of a membrane-embedded acceptor probe (Figure 8D). Oocytes labeled with only $DiIC_{12}(3)$ did not show any fluorescence when excited at the donor excitation wavelength of 491 nm, supporting the suitability of this probe as an acceptor fluorophore for AF. To ensure the presence of $DiIC_{12}(3)$ in the membrane, we visualized its presence using confocal microscopy and found a pericellular pattern, consistent with plasma membrane labeling (Figure S1 of the Supporting Information).

FRET between AF-labeled AE1(Q434C)·AE1-C$^-$ and bilayer-associated $DiIC_{12}(3)$ was measured (Figure 9). Fluorescence values of AF from oocytes expressing AE1·AE1-C$^-$ were used as background fluorescence, which were subtracted during the calculation of FRET efficiency (Figure 9). Oocytes expressing AE1-(Q434C)·AE1-C$^-$ exhibited a high level of FRET as reflected by the 72 ± 1% of Alexa Fluor 488 C_5-maleimide fluorescence quenching. The high efficiency of energy transfer suggested that AF, labeled at Q434C, and $DiIC_{12}(3)$, in the membrane, are close in space, at a distance shorter than the estimated Förster distance R_0 (33 Å) for the fluorophore pair.

DISCUSSION

In the absence of a crystal structure, structural insights into AE1 can be obtained only by alternate approaches. Distance constraints within AE1 will be important in evaluating any future

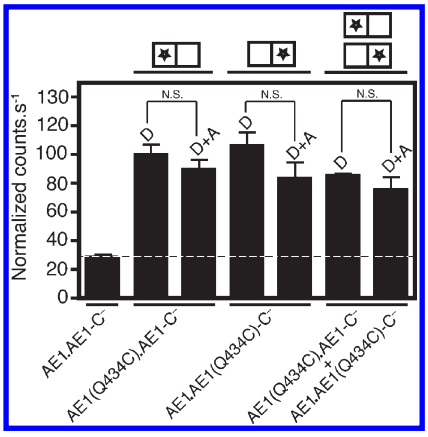

FIGURE 6: Measurement of the AE1·AE1 oligomeric state by FRET. Oocytes were injected with 75 ng of cRNA encoding AE1·AE1-C$^-$, AE1(Q434C)·AE1-C$^-$, or AE1·AE1(Q434C)-C$^-$ alone, and oocytes were coinjected with equal concentrations of AE1(Q434C)·AE1-C$^-$ and AE1·AE1(Q434C)-C$^-$. Three days postinjection, oocytes were treated with 1 mM 3-maleimidopropionic acid to block endogenous cysteines. Oocytes were then further incubated at 18 °C for one additional day to allow concatamer expression. On the fourth day, oocytes were incubated for 8 min in MBM, containing 270 μM AF (donor, D) and AF fluorescence emission was recorded at 520 nm, with an excitation wavelength of 475 nm. Oocytes were then incubated in MBM containing 350 μM TMR-MTS (acceptor, A) for 20 min, and the fluorescence was measured at an emission wavelength of 520 nm and an excitation wavelength of 475 nm. Spectra from three to nine oocytes were averaged and fluorescence counts measured in the presence of donor alone (D) and donor and acceptor (D+A) recorded. AF fluorescence from AE1·AE1-C$^-$ was taken as the background and is indicated by the dashed line. The fluorescence intensity was normalized by the value for AE1(Q434C)·AE1-C$^-$, with the donor alone. Above the bars are cartoons in which each pair of boxes represents a concatamer of AE1 and the star represents the AE1 subunit that contains the Q434C mutation. To determine whether FRET occurred between AF (donor, D) and TMR-MTS (acceptor, A), paired *t* tests were performed between fluorescence counts with D alone compared to D+A. The *p* value was greater than 0.05 in all cases and is indicated as N.S. (not significant).

crystal structure and assessing conformational changes that occur in AE1 during its transport cycle. To assess AE1 structurally and conformationally by FRET, we constructed a concatamer of two AE1 polypeptides joined head to tail, called AE1·AE1. The AE1 concatamer mimics the normal AE1 dimeric structure, but in a single polypeptide chain. AE1·AE1 has normal Cl^-/HCO_3^- exchange activity compared to that of wild-type AE1 and is processed to the plasma membrane when expressed in both HEK293 cells and *X. laevis* oocytes. Because AE1·AE1 did not associate into higher-order oligomers, FRET studies of AE1·AE1 will report energy transfer only within the concatameric unit. FRET measurements revealed a 49 Å distance between the two Q434 residues in the AE1·AE1 intramolecular dimer unit. Finally, the Q434 residue in the small extracellular loop between TM1 and TM2 was mapped within 33 Å of the lipid bilayer, on the basis of FRET efficiency.

AE1·AE1 was created for structural studies, but does it behave like wild-type AE1? When the concatamer was expressed in HEK293 cells, immunoblots showed that its expression level was similar to that of AE1. AE1·AE1 and AE1 also are processed to the cell surface to a similar degree in HEK293 cells and oocytes, indicating that AE1·AE1 is recognized like wild-type AE1 by the endoplasmic reticulum's biosynthetic apparatus and processing machinery of the Golgi apparatus. Because the Cl^-/HCO_3^- exchange activity of AE1·AE1 was indistinguishable from that of AE1 alone, we infer that the concatamer adopts a native structure in its membrane domains, which are solely responsible for transport function (*61*). The crystal structure of AE1 cytoplasmic domains reveals a dimer with a flexible unstructured cytoplasmic N-terminus (*8*). The AE1·AE1 concatamer was designed with the C-terminus of the first AE1 sequence fused to the second subunit with a two-residue linker. The presence of the AE1 N-terminus at the surface of the N-terminal domain [as indicated by the N-terminal domain crystal structure (*8*)] implies that the protein did not need to achieve a non-native fold to expose the N-terminus of the right AE1 subunit in the AE1 concatamer, so that it could be joined with the C-terminus of the left AE1 subunit. The ability of AE1 cytoplasmic domains to accommodate the stretch to join the AE1 subunits may have been enhanced by the high conformational flexibility of the N-terminal domain (*62*). The structure of the 43 kDa N-terminal cytoplasmic domain in the second AE1 subunit of AE1·AE1 may have been distorted, but this report does not assess the functionality of the cytoplasmic domains, whose role in erythrocytes is to anchor the plasma membrane to the cytoskeleton (*2*). Retention of AE1·AE1 functional activity is consistent with the fact that the Na^+/HCO_3^- cotransporter, NBC1 (SLC4A4), which is a member with AE1 of the SLC4A family, also is dimeric and is functional as a concatameric dimer (*63*). We conclude that AE1·AE1 membrane domains have native structure and therefore provide an appropriate background for structural studies.

Whether AE1·AE1 oligomerizes is a significant consideration for this study. FRET studies of AE1·AE1 are predicated on the ability to control positions of introduced cysteine residues within the AE1 dimeric unit that form the sites to introduce fluorescent probes. If AE1·AE1 oligmerizes, then FRET could occur between AE1·AE1 molecules, confounding the interpretation of FRET data. The minimal oligomeric state of AE1 is dimeric (*6*); AE1 monomers are strongly associated within the dimeric unit, such that denaturation is required to dissociate them (*32*). In erythrocytes, AE1 dimers and tetramers are found in a ratio of 60:40 (*64*). Tetramers are associated with the cytoskeleton, suggesting a role of cytoskeletal attachment in formation of tetrameric AE1 (*6*). Nondenaturing gel electrophoresis revealed that AE1·AE1 from HEK293 cells was exclusively monomeric, found only as unassociated concatamers. In FRET experiments, the transfer of energy between fluorescently labeled Q434C residues was examined. We found that between two Q434C residues, one in each AE1 unit, within a concatamer energy transfer occurred readily. In contrast, when AE1·AE1-C$^-$, with a Q434C mutation in either the left or right subunit, was expressed alone or coexpressed, no energy transfer was observed. We conclude that AE1·AE1 concatamers do not associate in a way that brings Q434C residues within 100 Å of each other. Because the AE1 dimer (and by implication AE1·AE1) is 110 Å long, we conclude that AE1·AE1 does not oligomerize when expressed in *X. laevis* oocytes. Finally, the expression level of AE1·AE1 in oocytes indicates that the protein's density in the membrane is too low for FRET to occur, unless the AE1·AE1 units associate into oligomers. The average distance between AE1·AE1 molecules is 200−300 Å, well beyond the 100 Å limit for FRET. Taken together, our results indicate that AE1·AE1 does not associate into oligomers when expressed in HEK293 cells or oocytes. Furthermore, AE1·AE1 can be used for FRET studies, and energy transfer will occur only within AE1·AE1 units.

For FRET studies, *X. laevis* oocytes were used to express introduced cysteine mutants in the AE1·AE1-C$^-$ background.

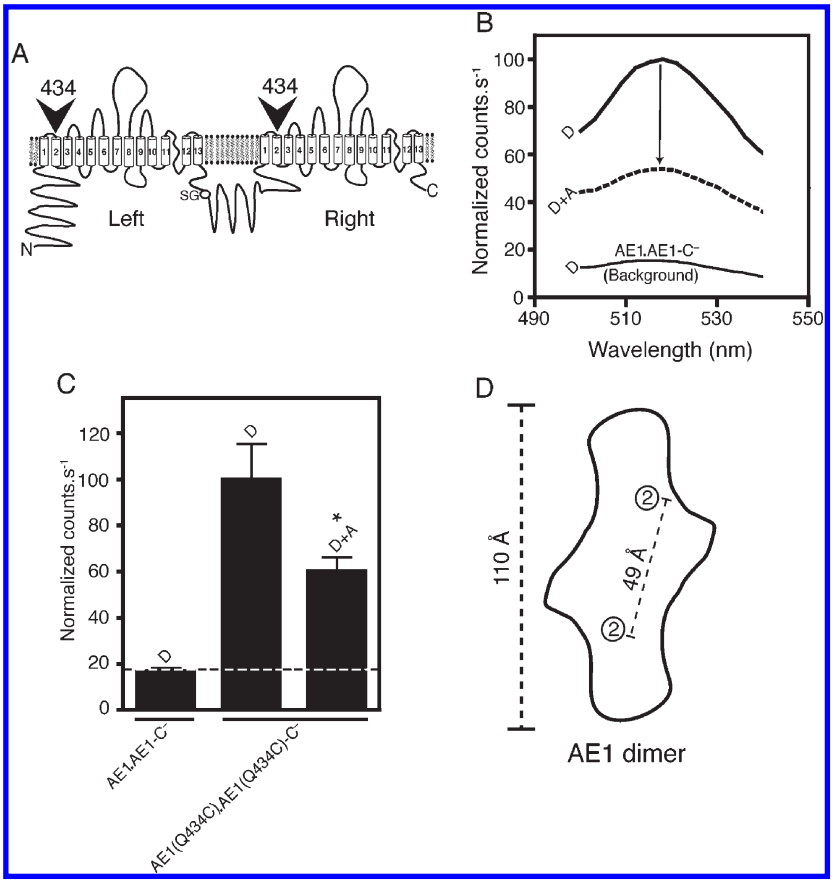

FIGURE 7: Distance between Q434 positions within an AE1 concatamer. (A) Cysteine residues were introduced at Q434 positions in the left and right subunits of AE1·AE1-C$^-$ (indicated by the arrows) to produce AE1(Q434C)·AE1(Q434C)-C$^-$. (B) Oocytes were treated with cRNA encoding AE1·AE1-C$^-$ and AE1(Q434C)·AE1(Q434C)-C$^-$. Three days postinjection, oocytes were treated with 1 mM 3-maleimidopropionic acid acid to block endogenous cysteines. Oocytes were then further incubated for an additional day at 18 °C to allow concatamer expression. On the fourth day, oocytes were incubated for 8 min in MBM containing 270 μM AF (donor, D) and the AF fluorescence emission spectrum was recorded over the 495−540 nm range, with an excitation wavelength of 475 nm. The same oocyte was then incubated in MBM containing 350 μM TMR-MTS (acceptor, A) for 20 min followed by a fluorescence scan under the conditions as described above. Fluorescence scans were recorded in the presence of donor alone (D) and donor and acceptor (D+A) for AE1(Q434C)·AE1(Q434C)-C$^-$. The background fluorescence was assessed for AE1·AE1-C$^-$-expressing oocytes, labeled with D only (bottom curve). (C) Fluorescence intensity at the peak fluorescence emission wavelength (520 nm) determined for AE1·AE1-C$^-$ and AE1(Q434C)·AE1(Q434C)-C$^-$. Paired *t* tests were performed to determine whether there was a statistically significant difference between fluorescence counts with D alone compared to D and A, which revealed $p < 0.02$ as indicated by the asterisk. (D) Outline map of the AE1 dimer, based upon a model determined by cryoelectron microscopy (*71*), shown with a possible position of TM2, indicated as labeled circles. FRET estimated the intersubunit C434−C434 distance to be 49 Å, as indicated by the scale bar.

Oocytes have been used for similar studies in the past (*65*, *66*), because they provide an expression system that can be readily physically manipulated (oocytes are 1 mm in diameter) and expresses membrane proteins readily (*66*, *67*). Here we found that AE1·AE1 was expressed at high levels, 1.2×10^{10} copies/oocyte, which is similar to the expression levels of other membrane proteins (*53*, *54*). Interestingly, this is the first report we can find that quantified the number of AE1 molecules expressed in an oocyte. AE1-mediated Cl^- fluxes in oocytes (*7*) combined with our measurement of AE1 expression level in the oocyte suggest that in oocytes AE1 turnover is 15−50-fold slower than in erythrocytes, where its rate of turnover is 10^5 s^{-1} (*25*). Optimal AE1 activity depends on interaction with a particular range of lipids (*68*, *69*) that may not be found in the oocyte membrane. Also, AE1 may require activation by kinases that are absent from oocytes. Finally, AE1 Cl^-/HCO_3^- exchange activity increases upon interaction with carbonic anhydrase II (*70*), which is not found in oocytes.

In FRET studies, the ability of cysteine residues endogenous to the oocytes to react with fluorescent probes was suppressed by treatment with 3-maleimidopropionic acid. Subsequently, expression of AE1·AE1 was allowed to proceed for another day before oocytes were labeled with cysteine-directed fluorescent probes and FRET studies were performed. The blocking procedure, which has been used previously (*57*), was successful in reducing background fluorescence (as reported by oocytes expressing AE1·AE1-C$^-$) to less than 20% of the fluorescence of cells expressing AE1(Q434C)·AE1-C$^-$.

To measure distances in AE1·AE1, we used the Q434C mutants. This residue is located in the first extracellular loop of AE1 (*15*) and was cloned into AE1·AE1-C$^-$ to generate AE1-(Q434C)·AE1(Q434C)-C$^-$. On the basis of FRET efficiency, the distance between Q434 residues within the AE1 dimer is 49 Å. The distance is reasonable in the context of what is known about AE1 structure. A two-dimensional projection map of the AE1 dimer, with dimensions of 60 Å × 110 Å (*16*, *71*), readily accommodates a Q434−Q434 distance of 49 Å. Cross-linking of introduced cysteine mutants and studies of coexpressed transmembrane segments of AE1 suggested that extracellular loop 1 is relatively close to the dimeric interface (*10*, *34*, *72*). Cross-linking of the two T431C residues in an AE1 dimer revealed that the residues must be able to come within 28 Å of each other (*34*).

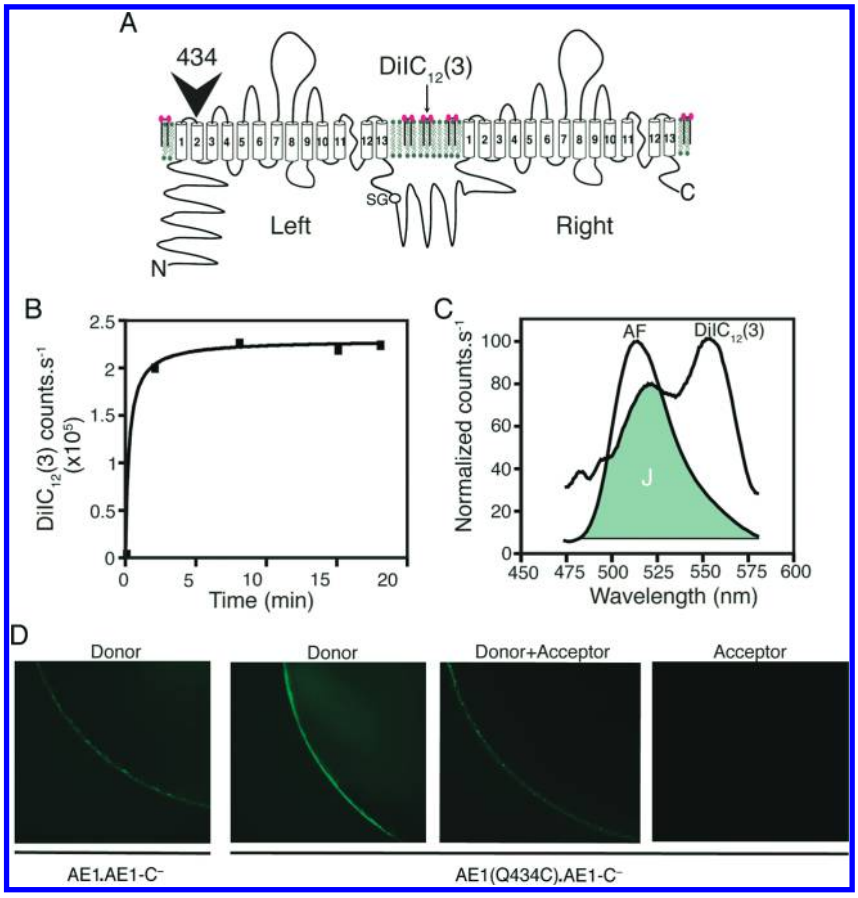

FIGURE 8: FRET between AE1(Q434C)·AE1-C$^-$ and the oocyte plasma membrane. (A) A single cysteine was introduced at the Q434 position of the left subunit of AE1·AE1-C$^-$ (indicated by the arrow) to produce AE1(Q434C)·AE1-C$^-$. DiIC$_{12}$(3) (purple dots) was incorporated into the oocyte plasma membrane. (B) Fluorescence labeling time curve for the *X. laevis* oocyte membrane by DiIC$_{12}$(3) monitored by excitation at 505 nm. The fluorescence emission at 585 nm was plotted vs incubation time and fitted with an exponential function. (C) Overlap (colored gray) of the Alexa Fluor 488 C_5-maleimide (AF) emission spectrum and the DiIC$_{12}$(3) excitation spectrum recorded for one oocyte. The integral of the overlap is denoted as *J*. (D) Confocal microscopy images of oocytes expressing (from left to right) AE1·AE1-C$^-$ labeled with Alexa Fluor 488 C_5-maleimide (donor), AE1(Q434C)·AE1-C$^-$ labeled with Alexa Fluor 488 C_5-maleimide (donor), AE1(Q434C)·AE1-C$^-$ labeled with Alexa Fluor 488 C_5-maleimide and DiIC$_{12}$(3) (donor+acceptor), and AE1(Q434C)·AE1-C$^-$ labeled with DiIC$_{12}$(3) (acceptor).

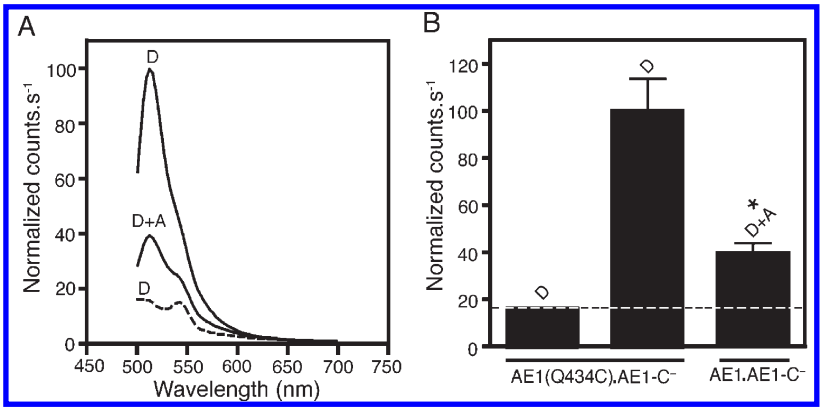

FIGURE 9: Measurement of FRET between AE1(Q434C)·AE1-C$^-$ and the plasma membrane of oocytes. (A) Average fluorescence emission from six oocytes expressing AE1(Q434C)·AE1-C$^-$, labeled with AF (D) or AF and DiIC$_{12}$(3) (D+A). Endogenous fluorescence from AE1·AE1-C$^-$ labeled with AF was also recorded (dashed line, D). (B) Average fluorescence from oocytes expressing AE1(Q434C)·AE1-C$^-$ labeled with AF and DiIC$_{12}$(3) (D+A) or AF (D) compared with average endogenous fluorescence from oocytes expressing AE1·AE1-C$^-$ labeled with AF. Fluorescence emission was recorded at 520 nm. A paired *t* test was performed to determine whether there was a statistically significant difference between fluorescence counts from oocytes expressing AE1(Q434C)·AE1-C$^-$ labeled with D alone compared to D and A ($p < 0.04$) as indicated by the asterisk.

Because chemical cross-linking covalently traps the nearest approach of two residues, it may be that AE1 can adopt rare conformations that bring these residues within 28 Å of each other. We have modeled possible positions of Q434 within the AE1 dimer, taking into account their 49 Å separation and the relative proximity of the residue to the lipid bilayer (Figure 7D). Without knowing the position of the dimeric interface within the two-dimensional projection map, we found Q434 residues could be in a range of possible sites consistent with a 49 Å separation of the homologous positions in each of the AE1 monomers. The

49 Å Q434−Q434 distance can now be used to test any AE1 structural model.

The distance from Q434 to the lipid bilayer provides a second distance constraint. FRET efficiency between a single Q434C in the left subunit of AE1·AE1-C$^-$ [AE1(Q434C)·AE1-C$^-$], labeled with AF, and the lipid bilayer, labeled with the lipophilic dye $DiIC_{12}(3)$, revealed a distance of less than 33 Å. The measurement must be viewed with caveats. First, the FRET measurement represents FRET between AF on AE1 and multiple $DiIC_{12}(3)$ molecules. That is, the value represents an average of FRET between AE1 and the belt of lipid around AE1. We assumed that $DiIC_{12}(3)$ was randomly and homogenously distributed in the membrane. We also know that there was no clustering of AE1(Q434C)·AE1-C$^-$ protein molecules, allowing us to presume that the distance measured between the donor and acceptor depends upon the dimension of a single concatamer [60 Å × 110 Å (*16*)], and the position of the Q434C mutation within the protein molecule. Second, we consider our experimental system as planar, because the Q434C mutation is close to the membrane surface (*2*), according to the latest topology model, and the fluorescent moiety of $DiIC_{12}(3)$ is present at the membrane surface (and not buried in the membrane core) with a slight possibility of $DiIC_{12}(3)$ flipping to the inner leaflet (*60*). FRET in a planar distribution system, like the lipid bilayer, is a complex case in which the efficiency of donor quenching by the acceptor is influenced by two factors: the minimum distance between the donor/acceptor pair and the acceptor concentration in the bilayer (*51*). Here, we obtained optimal energy transfer by saturating the membrane with the acceptor fluorophores. An accurate measurement of the Q434C−$DiIC_{12}(3)$ distance would require measurements of FRET efficiency over a range of $DiIC_{12}(3)$ concentrations. The measured FRET efficiency was very high (72%), suggesting that the donor and acceptor fluorophores are very close. Considering R_0 represents the distance at which FRET efficiency is 50%, we can say that Q434 is located much less than the R_0 distance [33 Å for the AF/$DiIC_{12}(3)$ pair] from the lipid bilayer. An accurate measurement of the Q434C−$DiIC_{12}(3)$ distance would require measurements of FRET efficiency over a range of $DiIC_{12}(3)$ concentrations. The model for the location of Q434C in the AE1 dimer has Q434 located close to the lipid bilayer, reflecting this finding.

Finally, the data presented here show that AE1·AE1 can be used as a model for structural studies of AE1. Preservation of AE1 functional activity implies that AE1·AE1 has native structure. The FRET studies here demonstrate that AE1·AE1 is amenable to FRET studies of structure. The ultimate utility of AE1·AE1 may be in FRET studies in which one subunit is cysteine-less and the other has two Cys residues, between which FRET can be measured. Use of AE1·AE1 will enable FRET measurements of distance within an AE1 unit, without confounding the FRET signal resulting from FRET across the dimeric interface. That is, if one expressed AE1 alone (as opposed to AE1·AE1) with two Cys residues, then FRET could occur within the monomer, but also between the monomers in the dimeric unit. Similarly, one could map distances from a fixed position in one subunit to different positions in the other subunit. AE1·AE1 effectively allows for an intramolecular dimer in which FRET can be controlled closely.

Here we report two distance constraints in the structure of AE1: 49 Å separation between Q434 residues in the AE1 dimer and a distance of less than 33 Å separating Q434 and the lipid bilayer. These constraints can be used to test the validity of any model or crystal structure of AE1. The data were collected using a new system to characterize AE1 structure: an AE1 concatamer (AE1·AE1) with individual cysteine mutations, combined with FRET. We found that AE1·AE1 is functional, consistent with the maintenance of a native structure in the membrane domain, and that AE1·AE1 does not oligomerize. Together, these studies show that AE1·AE1 is suitable for studies of AE1 structure and conformation by FRET.

ACKNOWLEDGMENT

We thank Dr. Michael Jennings (University of Arkansas) for the IVF12 antibody. We appreciate the advice from Dr. Francisco Bezanilla (University of Chicago, Chicago, IL) and Dr. Itzhak Fishov (Ben-Gurion University of the Negev, Beer-Sheva, Israel). Dr. Nicolas Touret (University of Alberta) provided assistance with confocal microscope imaging.

SUPPORTING INFORMATION AVAILABLE

Incorporation of $DiIC_{12}(3)$ into oocyte membranes (Figure S1) and accessibility of the C-terminal epitope in AE1·AE1 to the IVF12 antibody (Figure S2). This material is available free of charge via the Internet at http://pubs.acs.org.

REFERENCES

1. Fairbanks, G., Steck, T. L., and Wallach, D. F. (1971) Electrophoretic analysis of the major polypeptides of the human erythrocyte membrane. *Biochemistry 10*, 2606–2617.
2. Cordat, E., and Casey, J. R. (2009) Bicarbonate transport in cell physiology and disease. *Biochem. J. 417*, 423–439.
3. Wang, D. N. (1994) Band 3 protein: Structure, flexibility and function. *FEBS Lett. 346*, 26–31.
4. Peters, L. L., Shivdasani, R. A., Liu, S. C., Hanspal, M., John, K. M., Gonzalez, J. M., Brugnara, C., Gwynn, B., Mohandas, N., Alper, S. L., Orkin, S. H., and Lux, S. E. (1996) Anion exchanger 1 (band 3) is required to prevent erythrocyte membrane surface loss but not to form the membrane skeleton. *Cell 86*, 917–927.
5. Southgate, C. D., Chishti, A. H., Mitchell, B., Yi, S. J., and Palek, J. (1996) Targeted disruption of the murine erythroid band 3 gene results in spherocytosis and severe haemolytic anaemia despite a normal membrane skeleton. *Nat. Genet. 14*, 227–230.
6. Casey, J. R., and Reithmeier, R. A. (1991) Analysis of the oligomeric state of Band 3, the anion transport protein of the human erythrocyte membrane, by size exclusion high performance liquid chromatography. Oligomeric stability and origin of heterogeneity. *J. Biol. Chem. 266*, 15726–15737.
7. Dahl, N. K., Jiang, L., Chernova, M. N., Stuart-Tilley, A. K., Shmukler, B. E., and Alper, S. L. (2003) Deficient HCO_3^- transport in an AE1 mutant with normal Cl^- transport can be rescued by carbonic anhydrase II presented on an adjacent AE1 protomer. *J. Biol. Chem. 278*, 44949–44958.
8. Zhang, D., Kiyatkin, A., Bolin, J. T., and Low, P. S. (2000) Crystallographic structure and functional interpretation of the cytoplasmic domain of erythrocyte membrane band 3. *Blood 96*, 2925–2933.
9. Cheung, J. C., and Reithmeier, R. A. (2005) Membrane integration and topology of the first transmembrane segment in normal and Southeast Asian ovalocytosis human erythrocyte anion exchanger 1. *Mol. Membr. Biol. 22*, 203–214.
10. Groves, J. D., and Tanner, M. J. (1999) Structural model for the organization of the transmembrane spans of the human red-cell anion exchanger (band 3; AE1). *Biochem. J. 344* (Part 3), 699–711.
11. Tanner, M. J. (1997) The structure and function of band 3 (AE1): Recent developments (review). *Mol. Membr. Biol. 14*, 155–165.
12. Sahr, K. E., Taylor, W. M., Daniels, B. P., Rubin, H. L., and Jarolim, P. (1994) The structure and organization of the human erythroid anion exchanger (AE1) gene. *Genomics 24*, 491–501.
13. Fujinaga, J., and Casey, J. R. (1997) Topology studies of the membrane domain of the human erythrocyte anion exchanger, AE1. *Biophys. J. 72*, 198.
14. Fujinaga, J., Tang, X. B., and Casey, J. R. (1999) Topology of the membrane domain of human erythrocyte anion exchange protein, AE1. *J. Biol. Chem. 274*, 6626–6633.

15. Zhu, Q., Lee, D. W. K., and Casey, J. R. (2003) Novel Topology in C-terminal Region of the Human Plasma Membrane Anion Exchanger, AE1. *J. Biol. Chem. 278*, 3112–3120.
16. Wang, D. N., Sarabia, V. E., Reithmeier, R. A., and Kuhlbrandt, W. (1994) Three-dimensional map of the dimeric membrane domain of the human erythrocyte anion exchanger, Band 3. *EMBO J. 13*, 3230–3235.
17. Yamaguchi, T., Ikeda, Y., Abe, Y., Kuma, H., Kang, D., Hamasaki, N., and Hirai, T. (2010) Structure of the membrane domain of human erythrocyte anion exchanger 1 revealed by electron crystallography. *J. Mol. Biol. 397*, 179–189.
18. Huang, Y., Lemieux, M. J., Song, J., Auer, M., and Wang, D. N. (2003) Structure and mechanism of the glycerol-3-phosphate transporter from *Escherichia coli*. *Science 301*, 616–620.
19. Abramson, J., Smirnova, I., Kasho, V., Verner, G., Kaback, H. R., and Iwata, S. (2003) Structure and mechanism of the lactose permease of *Escherichia coli*. *Science 301*, 610–615.
20. Toyoshima, C., and Nomura, H. (2002) Structural changes in the calcium pump accompanying the dissociation of calcium. *Nature 418*, 605–611.
21. Toyoshima, C., and Inesi, G. (2004) Structural basis of ion pumping by Ca^{2+}-ATPase of the sarcoplasmic reticulum. *Annu. Rev. Biochem. 73*, 269–292.
22. Kuhlbrandt, W., Zeelen, J., and Dietrich, J. (2002) Structure, mechanism, and regulation of the *Neurospora* plasma membrane H^+-ATPase. *Science 297*, 1692–1696.
23. Stokes, D. L., and Green, N. M. (2003) Structure and function of the calcium pump. *Annu. Rev. Biophys. Biomol. Struct. 32*, 445–468.
24. Xu, C., Rice, W. J., He, W., and Stokes, D. L. (2002) A structural model for the catalytic cycle of Ca^{2+}-ATPase. *J. Mol. Biol. 316*, 201–211.
25. Jay, D., and Cantley, L. (1986) Structural aspects of the red cell anion exchange protein. *Annu. Rev. Biochem. 55*, 511–538.
26. Canfield, V. A., and Macey, R. L. (1984) Anion exchange in human erythrocytes has a large activation volume. *Biochim. Biophys. Acta 778*, 379–384.
27. Tang, X. B., and Casey, J. R. (1999) Protein chemical trapping of inhibitor-induced conformational changes in the erythrocyte membrane anion exchanger, AE1. *FASEB J. 13*, A1498.
28. Kuma, H., Shinde, A. A., Howren, T. R., and Jennings, M. L. (2002) Topology of the Anion Exchange Protein AE1: The Controversial Sidedness of Lysine 743. *Biochemistry 41*, 3380–3388.
29. Furuya, W., Tarshis, T., Law, F. Y., and Knauf, P. A. (1984) Transmembrane effects of intracellular chloride on the inhibitory potency of extracellular H_2DIDS. Evidence for two conformations of the transport site of the human erythrocyte anion exchange protein. *J. Gen. Physiol. 83*, 657–681.
30. Förster, T. (1959) Transfer mechanisms of electronic excitation. *Discuss. Faraday Soc. 27*, 7–17.
31. Stryer, L., and Haugland, R. P. (1967) Energy transfer: A spectroscopic ruler. *Proc. Natl. Acad. Sci. U.S.A. 58*, 719–726.
32. Boodhoo, A., and Reithmeier, R. A. F. (1984) Characterization of matrix-bound Band 3, the anion transport protein from human erythrocyte membranes. *J. Biol. Chem. 259*, 785–790.
33. Casey, J. R., Ding, Y., and Kopito, R. R. (1995) The role of cysteine residues in the erythrocyte plasma membrane anion exchange protein, AE1. *J. Biol. Chem. 270*, 8521–8527.
34. Taylor, A. M., Zhu, Q., and Casey, J. R. (2001) Cysteine-directed cross-linking localizes regions of the human erythrocyte anion exchange protein (AE1) relative to the dimeric interface. *Biochem. J. 359*, 661–668.
35. Sarkar, G., and Sommer, S. S. (1990) The megaprimer method of site-directed mutagenesis. *BioTechniques 8*, 404–407.
36. Bonar, P., and Casey, J. R. (2010) Purification of functional human Cl^-/HCO_3^- exchanger, AE1, over-expressed in *Saccharomyces cerevisiae*. *Protein Expression Purif. 74*, 106–115.
37. Graham, F. L., and van der Eb, A. J. (1973) A new technique for the assay of infectivity of human adenovirus 5 DNA. *Virology 52*, 456–467.
38. Penna, A., Demuro, A., Yeromin, A. V., Zhang, S. L., Safrina, O., Parker, I., and Cahalan, M. D. (2008) The CRAC channel consists of a tetramer formed by Stim-induced dimerization of Orai dimers. *Nature 456*, 116–120.
39. Laemmli, U. K. (1970) Cleavage of structural proteins during assembly of the head of bacteriophage T4. *Nature 227*, 680–685.
40. Jennings, M. L., Anderson, M. P., and Monaghan, R. (1986) Monoclonal antibodies against human erythrocyte Band 3 protein: Localization of proteolytic cleavage sites and stilbenedisulfonate-binding lysine residues. *J. Biol. Chem. 261*, 9002–9010.
41. Tang, X. B., Fujinaga, J., Kopito, R., and Casey, J. R. (1998) Topology of the region surrounding Glu681 of human AE1 protein, the erythrocyte anion exchanger. *J. Biol. Chem. 273*, 22545–22553.
42. Bradford, M. M. (1976) A rapid and sensitive method for the quantitation of microgram quantities of protein utilizing the principle of protein-dye binding. *Anal. Biochem. 72*, 248–254.
43. Soreq, H., Parvari, R., and Silman, I. (1982) Biosynthesis and secretion of catalytically active acetylcholinesterase in *Xenopus* oocytes microinjected with mRNA from rat brain and from *Torpedo* electric organ. *Proc. Natl. Acad. Sci. U.S.A. 79*, 830–834.
44. Leduc-Nadeau, A., Lahjouji, K., Bissonnette, P., Lapointe, J. Y., and Bichet, D. G. (2007) Elaboration of a novel technique for purification of plasma membranes from *Xenopus laevis* oocytes. *Am. J. Physiol. 292*, C1132–C1136.
45. Thomas, J. A., Buchsbaum, R. N., Zimniak, A., and Racker, E. (1979) Intracellular pH measurements in Ehrlich ascites tumor cells utilizing spectroscopic probes generated in situ. *Biochemistry 18*, 2210–2218.
46. Vilas, G. L., Johnson, D. E., Freund, P., and Casey, J. R. (2009) Characterization of an epilepsy-associated variant of the human Cl^-/HCO_3^- exchanger AE3. *Am. J. Physiol. 297*, C526–C536.
47. Li, M., Farley, R. A., and Lester, H. A. (2000) An intermediate state of the γ-aminobutyric acid transporter GAT1 revealed by simultaneous voltage clamp and fluorescence. *J. Gen. Physiol. 115*, 491–508.
48. Kim, S., Lakhani, V., Costa, D. J., Sharara, A. I., Fitz, J. G., Huang, L. W., Peters, K. G., and Kindman, L. A. (1995) Sphingolipid-gated Ca^{2+} release from intracellular stores of endothelial cells is mediated by a novel Ca^{2+}-permeable channel. *J. Biol. Chem. 270*, 5266–5269.
49. Koch, H. P., Kurokawa, T., Okochi, Y., Sasaki, M., Okamura, Y., and Larsson, H. P. (2008) Multimeric nature of voltage-gated proton channels. *Proc. Natl. Acad. Sci. U.S.A. 105*, 9111–9116.
50. Selvin, P. R. (1995) Fluorescence resonance energy transfer. *Methods Enzymol. 246*, 300–334.
51. Lakowicz, J. R. (2006) Principles of Fluorescence Spectroscopy, Springer, Berlin.
52. Koch, H. P., and Larsson, H. P. (2005) Small-scale molecular motions accomplish glutamate uptake in human glutamate transporters. *J. Neurosci. 25*, 1730–1736.
53. Wadiche, J. I., Arriza, J. L., Amara, S. G., and Kavanaugh, M. P. (1995) Kinetics of a human glutamate transporter. *Neuron 14*, 1019–1027.
54. Eskandari, S., Loo, D. D., Dai, G., Levy, O., Wright, E. M., and Carrasco, N. (1997) Thyroid Na^+/I^- symporter. Mechanism, stoichiometry, and specificity. *J. Biol. Chem. 272*, 27230–27238.
55. Quilty, J. A., Cordat, E., and Reithmeier, R. A. (2002) Impaired trafficking of human kidney anion exchanger (kAE1) caused by hetero-oligomer formation with a truncated mutant associated with distal renal tubular acidosis. *Biochem. J. 13*, 895–903.
56. Casey, J. R., and Reithmeier, R. A. F. (1990) HPLC gel filtration analysis of oligomeric structure of Band 3, the anion exchange protein of the erythrocyte membrane. *Biophys. J. 57*, 95a.
57. Posson, D. J., Ge, P., Miller, C., Bezanilla, F., and Selvin, P. R. (2005) Small vertical movement of a K^+ channel voltage sensor measured with luminescence energy transfer. *Nature 436*, 848–851.
58. Mukherjee, S., Soe, T. T., and Maxfield, F. R. (1999) Endocytic sorting of lipid analogues differing solely in the chemistry of their hydrophobic tails. *J. Cell Biol. 144*, 1271–1284.
59. Davey, A. M., Krise, K. M., Sheets, E. D., and Heikal, A. A. (2008) Molecular perspective of antigen-mediated mast cell signaling. *J. Biol. Chem. 283*, 7117–7127.
60. Wolf, D. E. (1985) Determination of the sidedness of carbocyanine dye labeling of membranes. *Biochemistry 24*, 582–586.
61. Grinstein, S., Ship, S., and Rothstein, A. (1978) Anion transport in relation to proteolytic dissection of band 3 protein. *Biochim. Biophys. Acta 507*, 294–304.
62. Thevenin, B. J., Periasamy, N., Shohet, S. B., and Verkman, A. S. (1994) Segmental dynamics of the cytoplasmic domain of erythrocyte band 3 determined by time-resolved fluorescence anisotropy: Sensitivity to pH and ligand binding. *Proc. Natl. Acad. Sci U.S.A. 91*, 1741–1745.
63. Kao, L., Sassani, P., Azimov, R., Pushkin, A., Abuladze, N., Peti-Peterdi, J., Liu, W., Newman, D., and Kurtz, I. (2008) Oligomeric structure and minimal functional unit of the electrogenic sodium bicarbonate cotransporter NBCe1-A. *J. Biol. Chem. 283*, 26782–26794.
64. Van Dort, H. M., Moriyama, R., and Low, P. S. (1998) Effect of band 3 subunit equilibrium on the kinetics and affinity of ankyrin binding to erythrocyte membrane vesicles. *J. Biol. Chem. 273*, 14819–14826.
65. Dempski, R. E., Hartung, K., Friedrich, T., and Bamberg, E. (2006) Fluorometric measurements of intermolecular distances between the α- and β-subunits of the Na^+/K^+-ATPase. *J. Biol. Chem. 281*, 36338–36346.

66. Chanda, B., Asamoah, O. K., Blunck, R., Roux, B., and Bezanilla, F. (2005) Gating charge displacement in voltage-gated ion channels involves limited transmembrane movement. *Nature 436*, 852–856.
67. Koch, H. P., Hubbard, J. M., and Larsson, H. P. (2007) Voltage-independent sodium-binding events reported by the 4B-4C loop in the human glutamate transporter excitatory amino acid transporter 3. *J. Biol. Chem. 282*, 24547–24553.
68. Maneri, L. R., and Low, P. S. (1988) Structural stability of the erthrocyte anion transporter, Band 3, in different lipid environments. *J. Biol. Chem. 263*, 16170–16178.
69. Maneri, L. R., and Low, P. S. (1989) Fatty acid composition of lipids which copurify with Band 3. *Biochem. Biophys. Res. Commun. 159*, 1012–1019.
70. Sterling, D., Reithmeier, R. A., and Casey, J. R. (2001) A Transport Metabolon. Functional Interaction of Carbonic Anhydrase II and Chloride/Bicarbonate Exchangers. *J. Biol. Chem. 276*, 47886–47894.
71. Wang, D. N., Kuhlbrandt, W., Sarabia, V., and Reithmeier, R. A. F. (1993) Two-dimensional structure of the membrane domain of human band 3, the anion transport protein of the erythrocyte membrane. *EMBO J. 12*, 2233–2239.
72. Casey, J. R. (2006) Why bicarbonate? *Biochem. Cell Biol. 84*, 930–939.